



NAM

Groningen Dynamic Model Update 2023

Anke Jannie Landman

NAM

Datum May 2023

Editors Jan van Elk

General Introduction

The subsurface model of the Groningen field is used to model the first step in the causal chain from gas production to induced earthquake damage and risk. It models the pressure response to the gas extraction in the gas and water bearing reservoir formations. Pressure decline in the field is an important driver for compaction and therefore subsidence. Compaction in turn affects stress and strain and is therefore of importance for the mechanism inducing earthquakes.

The reservoir model of the Groningen field was built in 2011 and 2012 and has a very detailed description of the faults in the field to support studies into induced earthquakes. The model was used to support Winningsplan 2013 (Ref. 1 to 3) and has since then been continuously improved (Ref. 4, 5, 7 and 8). This report describes the continuous improvement of the subsurface model of the Groningen field and in particular the effort to update and improve the history match.

For Winningsplan 2013 (Ref. 2) and Winningsplan 2016, the model was reviewed by the independent consultant SGS Horizon. For the review of the model for Winningsplan 2016, an extensive assurance report with opinion letter (Ref. 6) has been prepared by SGS Horizon.

The latest update of the reservoir model focussed on improving the model for forecasting the development of the pressure after gas production from the field has ceased, when initially intra-field pressure equilibration and later the response of lateral aquifers will dominate.

References

1. Winningsplan Groningen 2013, Nederlandse Aardolie Maatschappij BV, 29th November 2013.
2. Technical Addendum to the Winningsplan Groningen 2013; Subsidence, Induced Earthquakes and Seismic Hazard Analysis in the Groningen Field, Nederlandse Aardolie Maatschappij BV (Jan van Elk and Dirk Doornhof, eds), November 2013.
3. Supplementary Information to the Technical Addendum of the Winningsplan 2013, Nederlandse Aardolie Maatschappij BV (Jan van Elk and Dirk Doornhof, eds), December 2013.
4. Technical Addendum to the Winningsplan Groningen 2016 (chapter 1-5), Nederlandse Aardolie Maatschappij BV (Jan van Elk and Dirk Doornhof, eds), April 2016.
5. Groningen Field Review 2015 Subsurface Dynamic Modelling Report, Burkitov, Ulan, Van Oeveren, Henk, Valvatne, Per, May 2016.
6. Independent Review of Groningen Subsurface Modelling Update for Winningsplan 2016, SGS Horizon, July 2016.
7. Groningen Dynamic Model Update 2018, NAM, Henk van Oeveren, Per Valvatne and Leendert Geurtsen, September 2017
8. Groningen Dynamic Model Update 2019, Quint de Zeeuw and Leendert Geurtsen, NAM, October 2018.



NAM

| | | | |
|---|---|---------------------|-------------|
| Title | Groningen Dynamic Model Update 2023 | Date | May 2023 |
| | | Initiator | NAM |
| Autor(s) | Anke Jannie Landman | Editors | Jan van Elk |
| Organisation | NAM | Organisation | NAM |
| Place in the Study and Data Acquisition Plan | <p><u>Study Theme: Prediction Reservoir Pressure based on gas withdrawal</u></p> <p><u>Comment:</u></p> <p>The subsurface model of the Groningen field is used to model the first step in the causal chain from gas production to induced earthquake damage and risk. It models the pressure response to the gas extraction in the gas and water bearing reservoir formations. Pressure decline in the field is an important driver for compaction and therefore subsidence. Compaction in turn affects stress and strain and is therefore of importance for the mechanism inducing earthquakes.</p> <p>The reservoir model of the Groningen field was built in 2011 and 2012 and has a very detailed description of the faults in the field to support studies into induced earthquakes. The model was used to support Winningsplan 2013 and has since then been continuously improved. This report describes the continuous improvement of the subsurface model of the Groningen field and in particular the effort to update and improve the history match.</p> <p>For Winningsplan 2013 and Winningsplan 2016, the model was reviewed by the independent consultant SGS Horizon. For the review of the model for Winningsplan 2016, an extensive assurance report with opinion letter has been prepared by SGS Horizon.</p> <p>The latest update of the reservoir model focussed on improving the model for forecasting the development of the pressure after gas production from the field has ceased, when initially intra-field pressure equilibration and later the response of lateral aquifers will dominate.</p> | | |
| Directly linked research | <ul style="list-style-type: none"> • Reservoir Compaction • Optimisation of the aerial distribution of production | | |
| Used data | Sub-surface data from the Groningen field; open-hole logs, core data, pressure data, production data etc. | | |
| Associated organisation | Independent consultant SGS Horizon. | | |

| | |
|------------------|---|
| Assurance | For Winningsplan 2013 and Winningsplan 2016, the model was reviewed by an independent consultant SGS Horizon. |
|------------------|---|



NAM

Nederlandse Aardolie Maatschappij B.V.

Groningen Dynamic Model Update V7

Date: June 2023

Author: Anke Jannie Landman and Clemens Visser

EP number: EP202306200914

| Name | Ref. Indicator | Role | Date |
|---------------|----------------|---------------------------|------------|
| Hein de Groot | NAM-UPC/T/TS | Reservoir Engineering TA2 | 22/06/2023 |

1 Executive summary

This report describes the update and calibration of the Groningen dynamic reservoir model to version V7, completed early 2023. The dynamic model is used to generate pressure output that serves as input for subsidence and seismic risk studies. Therefore, the main objective of the model update was to obtain a good match in every region to the most recent pressure data.

The V6 model still provided a good match to most of the recently acquired SPG data, except for the Kolham-1 observation well. Special attention has been given to the Kolham and South-West periphery area. In addition, the following recommendations from the V6 model report have been implemented:

- Corrections of Ten Boer and Ameland layer thickness modelling in the static model
- Implementation of a Paleo contact for gas-in-aquifer
- Improvement of local mismatches:
 - BDM-5 SPG
 - DZL-1 PNL
 - Borgsweer SPG

The V6 model update was carried out in 2018. The following new data has since become available and was used for the V7 history-match:

- Additional SPG data (up to May-2022)
- Additional CiTHP data (up to May 2022)
- PNL data (from 2018 and 2020)
- LTMG (long-term memory gauge) pressure data Loppersum clusters (LRM, OVS, PAU, ZND)
- Additional strain data from the ZRP-3 DSS: cumulative strain with respect to May-2016 after 1, 2, 3, 4, and 5 years (V6 used a single data set of Nov-2017)
- Subsidence from 2018 survey compared to 1972 (V6 used 2013 survey)

Table 1 compares the V6 and V7 model history-match quality for the same datasets and metrics (unless otherwise specified). The model update was considered successful if an improved or similar match was obtained compared to V6. This was achieved for all datasets. The SPG data is considered the most important data set. The quality of the V7 SPG history-match in each of the Groningen pressure monitoring regions is compared to that of V6 in Table 2 and Figure 1.

Introducing a new Borgsweer fault seal factor enabled improvement of the match to Borgsweer pressure and DZL-1 water encroachment at the same time. The now excellent match of the rise of the GWC in DZL-1 is one of the V7 model highlights. The V7 model matches both the early and late pressure data for KHM-1 very well, including a recently acquired pressure that was not used in the calibration.

Table 1: Field-wide history match quality for the V6 and V7 models, described by the RMSE (Root Mean Square Error) to the data.¹

| Data set | Unit | RMSE V6 | RMSE V7 |
|-------------------------|----------------------------|---------|-------------------|
| SPG | bar | 2.8 | 2.3 |
| PNL (interpreted GWC) | m | 10.4 | 8.6 |
| RFT | bar | 9.8 | 7.4 |
| CiTHP | bar | 1.9 | 1.8 |
| Subsidence ² | cm | 2.1 | 2.4 |
| Strain ZRP-3 | ($\mu\text{m}/\text{m}$) | 24.2 | 18.8 ³ |
| Gravity (All) | (μGal) | 5.0 | 5.1 |
| Gravity (Carboniferous) | (μGal) | 7.9 | 7.6 |

Table 2: SPG RMSE for the Groningen pressure monitoring regions.

| Region | RMSE V6 | RMSE V7 |
|----------------------|---------|---------|
| South-West Periphery | 3.4 | 3.0 |
| South-West | 1.4 | 1.3 |
| North-West | 1.8 | 1.5 |
| North-East | 1.7 | 1.2 |
| Central-East | 1.3 | 1.4 |
| South-East | 2.5 | 2.3 |
| South-Central | 1.9 | 1.7 |

¹ Details on the RMSE calculations can be found in Section 4.3.

² Using C_m -porosity relation for both V6 and V7 models. V7 uses the 2018 survey, whereas V6 uses the 2013 survey, both in comparison to the 1972 survey.

³ Based on larger data set.

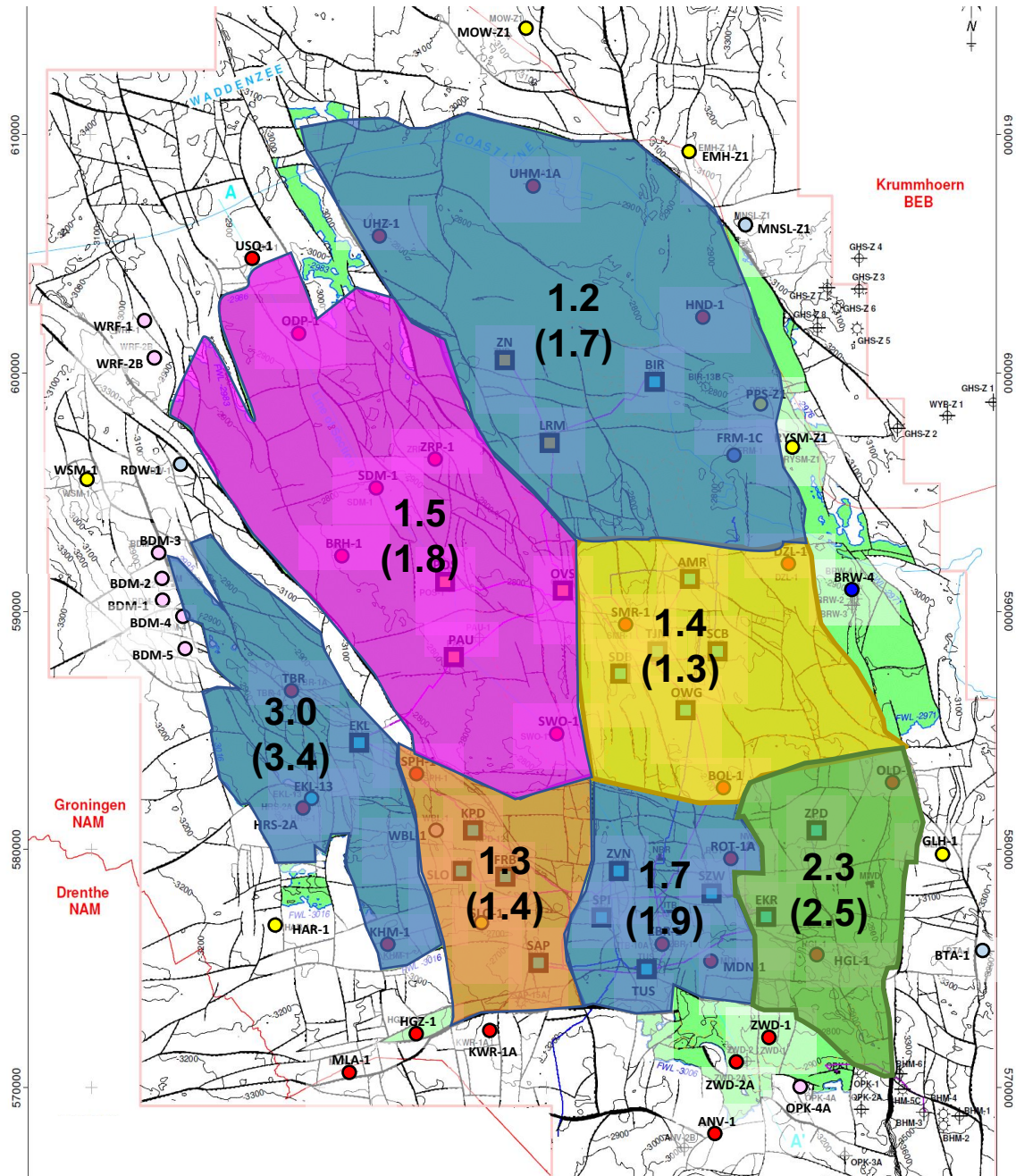


Figure 1: V7 and V6 (in brackets) model RMSE for SPG data in the Groningen monitoring regions.

Contents

| | | |
|-------|--|----|
| 1 | Executive summary | 2 |
| 2 | Introduction | 7 |
| 2.1 | Background and model objective | 7 |
| 2.2 | Report structure..... | 7 |
| 3 | Static Model | 8 |
| 3.1 | Introduction | 8 |
| 3.2 | Model grid architecture | 8 |
| 3.3 | Well position relative to faults..... | 9 |
| 3.4 | Continuity of the Ameland Claystone Member | 9 |
| 3.5 | Petrophysical modelling..... | 10 |
| 3.6 | Volumetric comparison..... | 10 |
| 3.7 | Upscaling for dynamic model | 10 |
| 4 | History Match Methodology..... | 12 |
| 4.1 | Workflow..... | 12 |
| 4.2 | Input variables | 14 |
| 4.2.1 | Grid block volume multipliers | 14 |
| 4.2.2 | Regional permeability multipliers | 14 |
| 4.2.3 | Carboniferous properties..... | 15 |
| 4.2.4 | Fault seal factors | 15 |
| 4.2.5 | Aquifer and aquifer pseudo-well properties..... | 16 |
| 4.2.6 | Relative permeability and fluid parameters | 17 |
| 4.2.7 | Gas-in-aquifer properties..... | 17 |
| 4.2.8 | Regional Free Water Levels..... | 18 |
| 4.2.9 | Rock compressibility | 19 |
| 4.3 | Response variables..... | 19 |
| 4.3.1 | SPG RMSE..... | 19 |
| 4.3.2 | RFT RMSE | 20 |
| 4.3.3 | CiTHP2BHP RMSE | 21 |
| 4.3.4 | PNL RMSE..... | 21 |
| 4.3.5 | Subsidence RMSE | 22 |
| 4.3.6 | DSS RMSE | 22 |
| 4.3.7 | Gravity RMSE..... | 23 |
| 4.4 | History-Match process..... | 23 |
| 5 | Model Adjustments and New Features | 25 |
| 5.1 | Kolham and Southwest periphery | 25 |

| | | |
|------------|--|----|
| 5.1.1 | Variables impacting Kolham pressure match | 25 |
| 5.1.2 | Gas-in-aquifer extension and Paleo contact | 29 |
| 5.1.3 | Kolham history-match | 30 |
| 5.2 | Bedum | 31 |
| 5.3 | Region North-East | 32 |
| 5.4 | Borgsweer and DZL-1 | 35 |
| 6 | History-Match Results | 38 |
| 6.1 | Overview | 38 |
| 6.1.1 | GIIP | 38 |
| 6.1.2 | Global history-match | 38 |
| 6.1.3 | Regional SPG pressure match | 39 |
| 6.2 | New SPG data | 39 |
| 6.3 | LTMG data Loppersum clusters | 40 |
| 6.4 | Carboniferous depletion | 41 |
| 6.5 | DSS data | 44 |
| 6.6 | Southern Lauwerszee Aquifer | 45 |
| 6.6.1 | Fault seal factors | 45 |
| 6.6.2 | Pseudo-aquifer wells | 47 |
| 6.7 | Subsidence match | 47 |
| 7 | Conclusions | 49 |
| 8 | References | 50 |
| Appendix A | V7 best match | 51 |
| Appendix B | History-Match input variable values | 52 |
| Appendix C | Conversion of CiTHP to BHP | 55 |
| Appendix D | Midlaren history-match | 56 |

2 Introduction

2.1 Background and model objective

This report describes the update and calibration of the Groningen dynamic reservoir model to version V7, completed early 2023. Because the Groningen field is operating on minimum flow, the Groningen dynamic model is no longer used for forecasting of production capacity. The modelling focus is now on reservoir pressure prediction. The dynamic model is used to generate pressure output that serves as input for subsidence and seismic risk studies. Therefore, the main objective of the model update was to obtain a good match in every region to the most recent pressure data.

The V6 model still provided a good match to most of the recently acquired SPG data, except for the Kolham-1 observation well. Special attention has been given to the Kolham and South-West periphery area. The following recommendations from the V6 model report [1] have been implemented:

- Corrections of Ten Boer and Ameland layer thickness modelling (See Chapter 3: Static Model)
- Implementation of a Paleo contact for gas-in-aquifer (See Section 5.1.2)
- Improvement of local mismatches:
 - BDM-5 SPG (Section 5.2)
 - DZL-1 PNL (Section 5.4)
 - Borgsweer SPG (Section 5.4)

The V6 model update was carried out in 2018. The following new data has since become available and was used for the V7 history-match:

- Additional SPG data (up to May-2022)
- Additional CiTHP data (up to May 2022)
- PNL data (from 2018 and 2020)
- LTMG (long-term memory gauge) pressure data Loppersum clusters (LRM, OVS, PAU, ZND)
- Additional strain data from the ZRP-3 DSS: cumulative strain with respect to. May-2016 after 1, 2, 3, 4, and 5 years (V6 used a single data set of Nov-2017)
- Subsidence from 2018 survey compared to 1972 (V6 used 2013 survey)

2.2 Report structure

Chapter 3 describes the modifications that have been made to the Groningen Petrel static model since dynamic model V6. Chapter 4 describes the history match workflow, the input variables, and the response variables used to quantify the history-match quality. Chapter 5 describes adjustments in the dynamic model to improve the match in certain regions. Chapter 6 discusses the most important results and the history-match quality. Chapter 7 summarizes the most important conclusions.

3 Static Model

3.1 Introduction

The Groningen V6 dynamic reservoir model was based on Version 6 of the static model of the Groningen field (Petrel_V.6). While running dynamic simulations with the Groningen V6 MoReS model, a few small issues were identified that could be traced back to equally small deficiencies in the 3D grid of Petrel_V.6. This triggered the building in 2018 of a static model Petrel_V.6.3.1 by Asad Ilyas, in which all identified issues were addressed and repaired. For consistency in naming of model versions, Petrel_V.6.3.1 will be referred to as Petrel_V.7 in this report. This chapter gives a brief overview of the changes applied to Petrel_V.6 to arrive at Petrel_V.7, which is the basis for dynamic model V7.

3.2 Model grid architecture

The Ten Boer Claystone interval is subdivided into three reservoir zones TBS.1, TBS.2 and TBS.3 which concordantly lie on top of the Slochteren sandstone reservoir units. In the southwest corner of Petrel_V.6 some issues were observed with the concordant architecture of the Ten Boer zones, resulting in local pinch-outs, discontinuities, and distortions of model layers. The cause turned out to be related to the fact that the top picks of the Ten Boer zones were missing in some of the wells in the area. Due to the absence of these control points, interpolation algorithms were not able to consistently impose concordant layering causing the issues described above. This was repaired by adding missing picks to the wells in question.

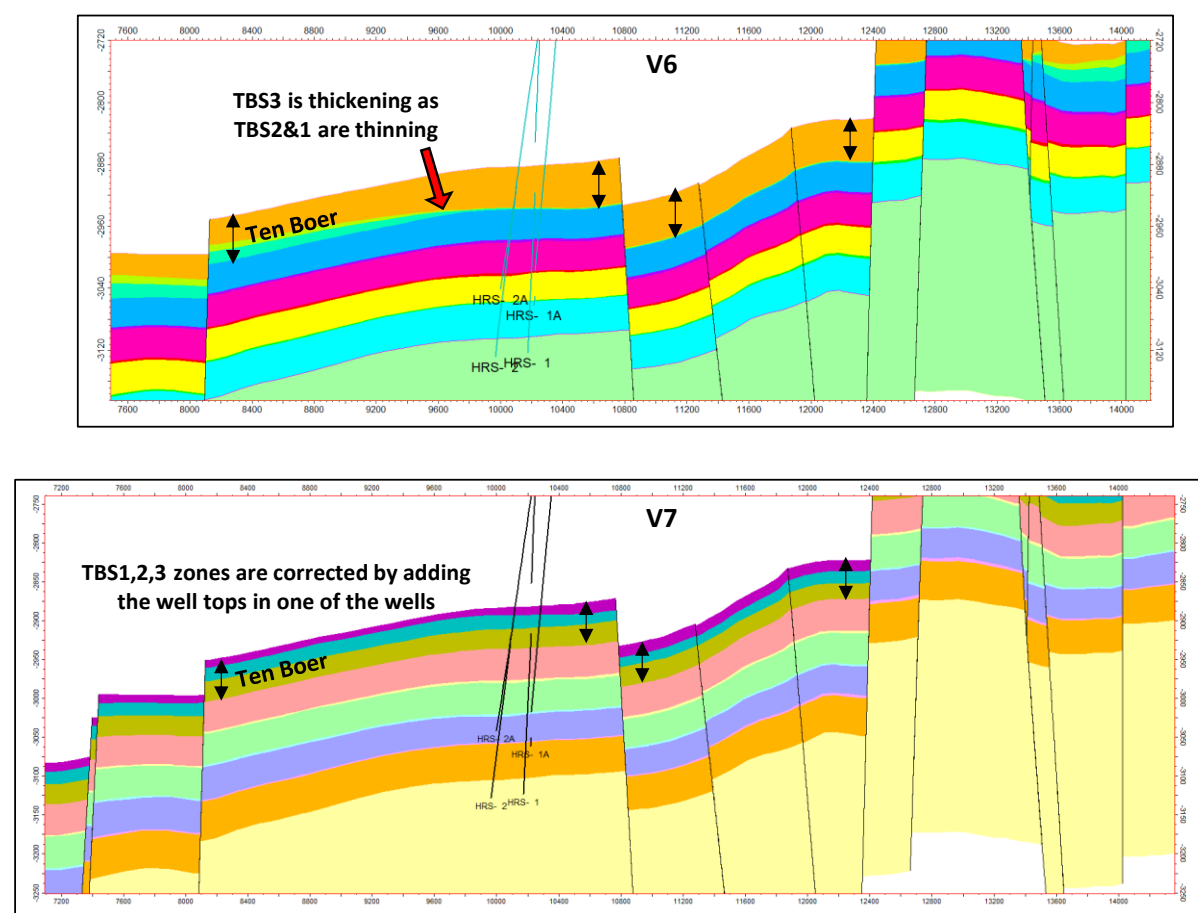


Figure 2: Intersection through HRS-2A showing the corrected Ten Boer zonation in Petrel_V7 (bottom) versus Petrel_V6 (top).

Figure 2 and Figure 3 show examples in the Harkstede and Bedum-5 areas, with zone architecture before and after resolution of the issue.

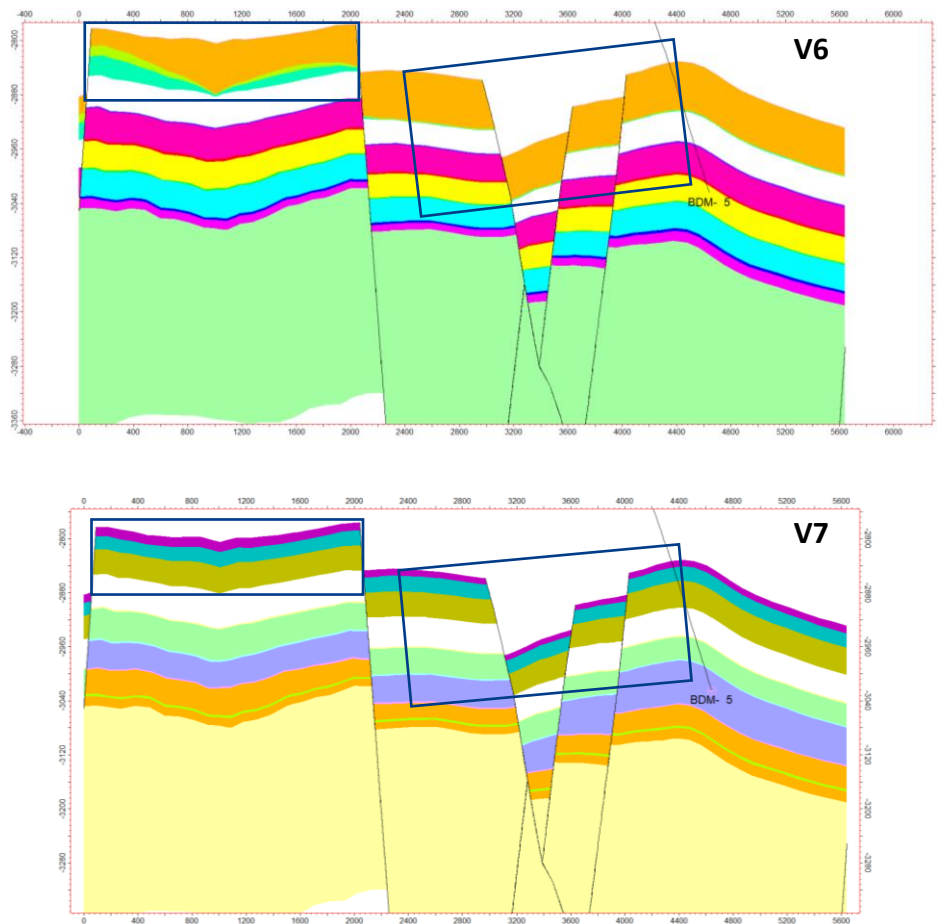


Figure 3: Intersection through BDM-5 showing the corrected Ten Boer zonation in Petrel_V7 (bottom) versus Petrel_V6 (top).

3.3 Well position relative to faults

An issue was observed with well EKR-204 in the De Eeker cluster in the south-eastern part of the Groningen field. The top of the Slochteren Sandstone in EKR-204 lies 20 m deeper than in neighbouring wells, indicating the presence of a small separating fault, though pressure data suggests full communication. A possible solution was to make a small adjustment to the local fault pattern. Fault position uncertainty in the cluster area is relatively large due to the presence of a thick salt dome in the overlying Zechstein interval. Changing fault positions could potentially have big consequences for rebuilding the model grid. Therefore, it was decided not to implement any changes in the fault pattern. A pragmatic solution had already been implemented in dynamic model V6 [1]. The position of well EKR-204 was shifted in the dynamic model to bring it to the other side of the small separating fault, such that EKR-204 lies in the same fault block as wells EKR-11, EKR-5, EKR-4A, and EKR-205. The same approach is used in dynamic model V7, with one correction. In the V6 model EKR-204 was perforated all the way down to within the Carboniferous zones, because the reservoir is 20 m shallower at its new position. In the V7 dynamic model this has been corrected by also adjusting the EKR-204 perforation depths by 20 m.

3.4 Continuity of the Ameland Claystone Member

Some unexpected variability was observed in the thickness distribution of the Ameland Claystone equivalent reservoir zone in the north-eastern part of the Groningen field. This was inspected by

checking well picks in all available wells in the area, particularly from the Bierum cluster. Minor adjustments were made to the picks in a few wells. This resulted in a more continuous Ameland zone with reduced lateral thickness variation which is expected to enhance the options in the dynamic realm to use the Ameland Claystone as a local baffle or barrier.

3.5 Petrophysical modelling

Various checks were carried out on the property modelling approach for Petrel_V.6. One check concerned with the incorporation of core analysis results from the Zeerijp-3A well. This well was drilled and cored in 2015 with results gradually becoming available in the course of 2016. It was confirmed that core analysis data were included in the determination of a porosity-permeability transform and that the porosity and gamma ray wireline logging data were included in the property modelling workflows.

Additional checks were carried out to confirm the robustness of the general property modelling approach (upscaling → de-trending → normalization → variogram analysis → petrophysical modelling). The V6 property modelling approach was left unchanged, but properties were repopulated after the structural model re-build.

3.6 Volumetric comparison

A deterministic base case GIIP was calculated for Petrel_V.7 to be 2870 Bcm. This is less than 1% different from the GIIP calculated for Petrel_V.6. The main reduction in GIIP is associated with the changes made in the layering of the Ten Boer Claystone. The difference for the Slochteren reservoir zones is slightly less than 0.2%.

3.7 Upscaling for dynamic model

The same upscaling approach is applied as in model V6. In horizontal direction the grid is upscaled by a factor 4. The degree of vertical upscaling is zone dependent. The number of layers in the static and upscaled model per reservoir zone are given in

Table 3. The Carboniferous is split into 8 zones with increasing thickness as found optimal for V6 [1].

Upscaling was performed in Reduce++ (Dynamo's upscaling package). A comparison was made of the Gross Rock Volume (GRV) of the Petrel model to that in Reduce++ after i) loading the complete model in Reduce++, ii) loading the model extent as used for the dynamic model, before upscaling, and iii) after upscaling. The GRV was conserved after loading in Reduce++. Since not all voxels of the static grid are used in the dynamic model this reduces the GRV by 1.6%, exactly like in the V6 model. The upscaling process (including voiding blocks) reduced the GRV with another 1% (compared to 2% in V6 and 4% in V5). The Net Rock Volume and Pore Volume are completely conserved in the upscaling process.

Table 3: Vertical upscaling from static to dynamic model by reservoir zone. USS and LSS denote Upper Slochteren (ROSLU) and Lower Slochteren (ROSLI).

| Zone ID | Zone Name | Number of layers fine grid | Number of layers coarse grid |
|-------------------------|-----------------|-------------------------------|---------------------------------|
| 0 | TBS3 | 10 | 1 |
| 1 | TBS2 | 10 | 1 |
| 2 | TBS1 | 20 | 1 |
| 3 | USS_3res | 15 | 3 |
| 4 | USS_2het | 4 | 1 |
| 5 | USS_2res | 20 | 6 |
| 6 | USS_1het | 4 | 1 |
| 7 | USS_1res | 20 | 5 |
| 8 | LSS_2het | 6 | 1 |
| 9 | LSS_2res | 30 | 7 |
| 10 | LSS_1het | 6 | 1 |
| 11 | LSS_1res | 30 | 6 |
| 12 | Carboniferous_8 | 1 | 1 |
| 13 | Carboniferous_7 | 2 | 1 |
| 14 | Carboniferous_6 | 4 | 1 |
| 15 | Carboniferous_5 | 8 | 1 |
| 16 | Carboniferous_4 | 11 | 1 |
| 17 | Carboniferous_3 | 11 | 1 |
| 18 | Carboniferous_2 | 11 | 1 |
| 19 | Carboniferous_1 | 12 | 1 |
| Total number of layers: | | 235 | 42 |

4 History Match Methodology

4.1 Workflow

This chapter describes the methodology used to obtain the V7 history-match. The principal workflow remains the same as for previous model updates, as described in the 2015 model update (V2.5) report [2]. It starts with a variety of model input variables that are used to modify properties of the dynamic model. The various types of input variables are described in Section 4.2. Each variable carries uncertainty and can take on a range of values. In practice only a very limited number of possible input variable value combinations can be simulated. A space-filling experimental design is used to generate the input data sets for a maximum of 1000 simulation runs at a time. Such a set can be run in about one week. The space-filling design aims to distribute the input variable value combinations optimally in the multi-dimensional space.

An example of a space filling design, for a simple case of only three input variables, is illustrated in three-dimensional space in Figure 4a. When 50 input variables are used, this space becomes 50-dimensional. The volume over which the points need to be distributed increases exponentially with the number of dimensions. This means that many more data points (corresponding to simulation runs) are then needed to fill the input variable space.

Figure 4b illustrates the simulation of a set of runs. Each simulation results in a set of calculated responses. These responses correspond to mismatch functions for each data set. The responses quantify the quality of the match between model and measured data. The goal is to find optimal input variable values to minimize the difference between the dynamic model outcome and the measurements. In other words, to minimize the response variables. The response variables are described in detail in Section 4.3.

New in this model update is the use of the Autosum tool. This tool has been developed in Shell as a collaborative effort between the subsurface and wells data science, the Quantitative Reservoir Management, and the Upstream Analytics teams. As illustrated in Figure 4c, a data table is loaded in the Autosum tool for analysis and modelling. Each row in the data table contains the input variable and response variable values of a single simulation run. Machine learning models in the Autosum tool allow modelling of the relationships between input and response variables. The loaded simulation data is used to train and test these models. The machine learning models give additional insights in the relationship between inputs and responses and help to decide on the choice of input variables and their ranges for subsequent simulation cycles. They can also be used for response prediction. To build machine learning models of sufficient quality, at least 20 data points (corresponding to simulation runs) are required for each input variable (“feature” in Autosum).

Section 4.4 describes how a series of these simulation and analysis cycles have been used to: i) determine the most significant features, ii) obtain a global history-match, and iii) improve the history-match regionally.

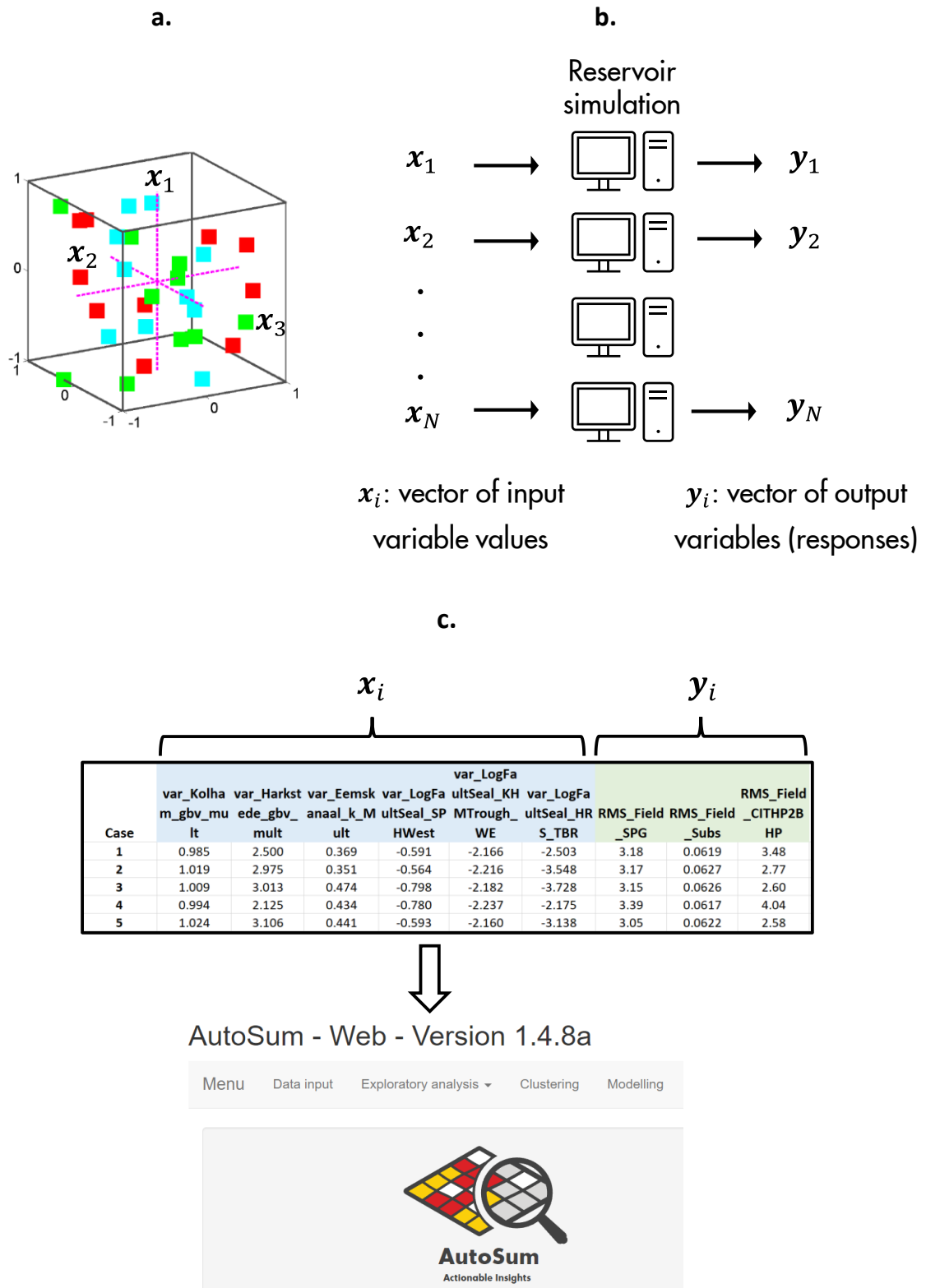


Figure 4: Illustration of history-matching workflow: a) A simple space filling design with only three input variables (three dimensions). b) An experimental design of N runs is simulated in Dynamo v. 2021.2. c) A table with input and simulated responses for the N runs is loaded in the AutoSum web tool for analysis and response proxy modelling.

4.2 Input variables

The V6 model update used about 120 history-match input variables (see Appendix B). These formed the starting point for the V7 model calibration. The input variables can be grouped as follows, and will be discussed in subsequent subsections:

- Grid block volume multipliers
 - 9 for regions of the Groningen field
 - 8 for other fields in the model (Usquert, Zuidwending East, Bedum, Kielwindeweer, Feerwerd, Warffum, Annerveen, Midlaren)
- Regional permeability multipliers
- Properties of the Carboniferous (Limburg group)
- Fault seal factors
- Aquifer and aquifer pseudo-well properties
- Relative permeability and fluid parameters
- Gas-in-aquifer properties
- Regional Free Water Levels
- Rock compressibility parameters

4.2.1 Grid block volume multipliers

The grid block volume (GBV) multipliers are applied on the Gross Rock Volume and thus adjust the amount of Gas Initially In Place (GIIP) directly. They capture the combined uncertainty in structure, porosity, and Net to Gross. An additional GBV multiplier has been introduced for the Bedum South field to improve the Bedum history-match, which is discussed in Section 5.2.

4.2.2 Regional permeability multipliers

For the V6 model update porosity-dependent permeability multipliers were introduced [1]. The reason for this is that there is relatively more variation in permeability at low porosity/permeability than for higher porosity/permeability values. A uniform multiplier on all permeabilities would not do this justice. The same approach is taken for V7, with updated relationships determined based on the distribution of permeabilities in the new model (Figure 5).

The following updated relationships are used for an increase in permeability ($\log_k_mult > 0$):

$$k_{adj} = k \cdot 10^{(-3.260\phi + 1.033) \cdot \log_k_mult}, \quad [\text{Eq. 1}]$$

and for a decrease in permeability ($\log_k_mult < 0$):

$$k_{adj} = k \cdot 10^{(4.118\phi - 1.440) \cdot \log_k_mult}. \quad [\text{Eq. 2}]$$

For none of the Groningen regions a decrease in permeability is required to achieve a history-match, so in practice only Equation 1 is used. A log-permeability multiplier of 0 leaves the permeability unadjusted. A log-permeability multiplier of 1 multiplies the grid block permeability by a factor equal to the ratio of the fitted P10 (high) and P50 (mid) permeability for the applicable porosity class. This translates into a range of permeability multiplication factors from 1.3 for very high porosity ($\phi = 0.28$) to 8.0 for very low porosity ($\phi = 0.04$). The Groningen dynamic models have consistently needed permeability multipliers to obtain a history-match. A key reason for this is that high permeability streaks that are seen in core and log data cannot be adequately captured in the upscaled model.

Log(k) versus Porosity
V7 Dynamic Model

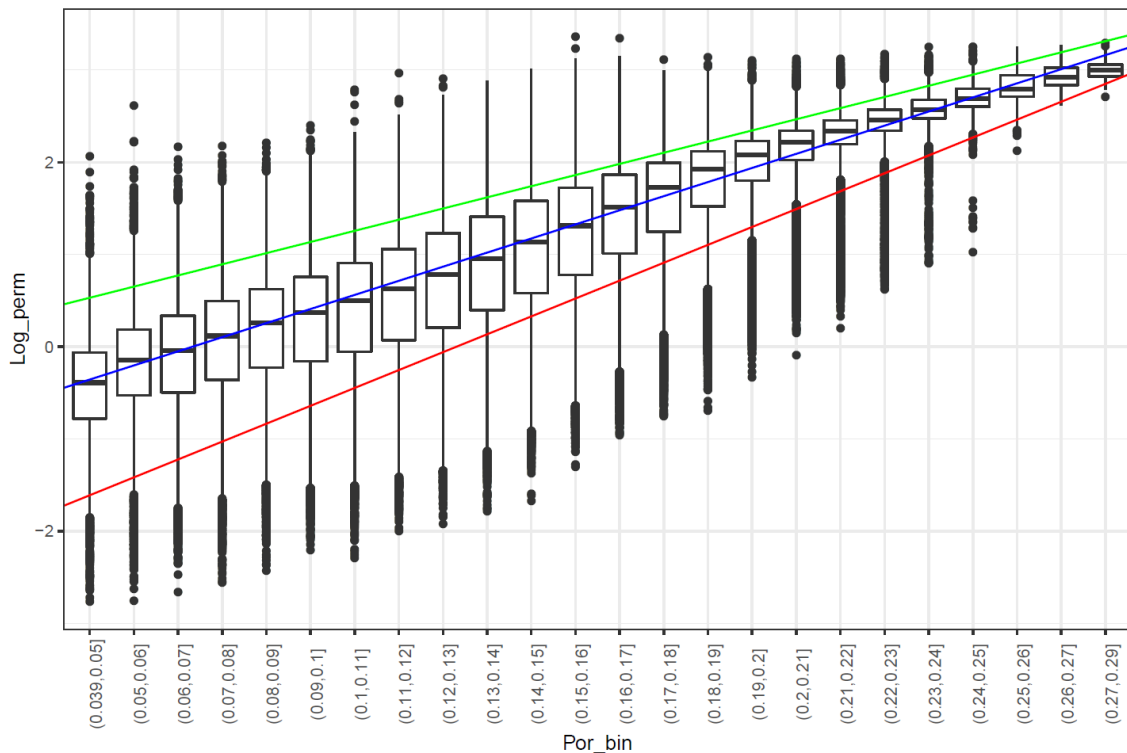


Figure 5: Box-and-whisker plot of gridblock permeability in the Rotliegend for each porosity bin. The lines correspond to a linear model fit to P10/P50/P90 permeability values.

4.2.3 Carboniferous properties

The Carboniferous super group was introduced in the V6 model as described in the V6 model report [1]. It is modelled with uniform properties that can be adjusted with a few input variables. The same five variables are still used:

- *Carboniferous_horizon_Mult*: reduces the transmissibility between the Slochteren reservoir and top Carboniferous in the same manner as a fault seal factor.
- *Carboniferous_por_mult*: multiplies the Carboniferous porosity, and therefore its GIIP.
- *Carboniferous_kvkh_Mult*: Carboniferous kvkh
- *Carboniferous_kh_Mult*: Carboniferous horizontal permeability multiplier
- *Compress_rock_Carb*: Carboniferous rock compressibility

An additional multiplier (*Compress_rock_Carb_Mult*) is introduced to be able to use a different compressibility value to calculate reservoir compaction and strain in ZRP-3A than is needed to match surface subsidence. Section 6.4 describes how the Carboniferous variables have been set to obtain the best match on pressure data.

4.2.4 Fault seal factors

The V6 model had transmissibility adjustments on 46 faults, extensively described in the model report [1]. The input variables are log fault seal factors ranging from -4 (transmissibility across fault multiplied by 10^{-4}) to 0 (fully open fault). An additional fault seal factor has been introduced in V7 to improve the Borgsweer pressure match. This is explained in Section 5.4.

4.2.5 Aquifer and aquifer pseudo-well properties

Analytical aquifer models are attached to the model grid boundaries for the Möwensteert, Rodewolt, Rysum, and Usquert aquifers. See Figure 6 for the locations of these aquifers. The size of these four aquifers can be set through model input variables. Another input variable acts as a multiplier on the aquifer water viscosity. Sensitivities on these aquifer input variables showed that their effect on the pressure history-match is insignificant compared to other variables. These five aquifer input variables have therefore been set equal to the V6 values and have not been used in the model calibration. See the table in Appendix B for their values.

The Southern Lauwerszee aquifer (denoted “Zuidelijke Lauwerszee Trog” in Figure 6) is connected to the Groningen field as well as to several other gas fields on its south-western side. In the V6 model, pseudo-aquifer wells were introduced to allow depletion of this aquifer resulting from gas production in the Faan, Pasop, Roden, and Vries fields. Figure 7 highlights these wells along the south-western model boundary.



Figure 6: The Groningen field and connected aquifers (in blue) and gas fields (in green).

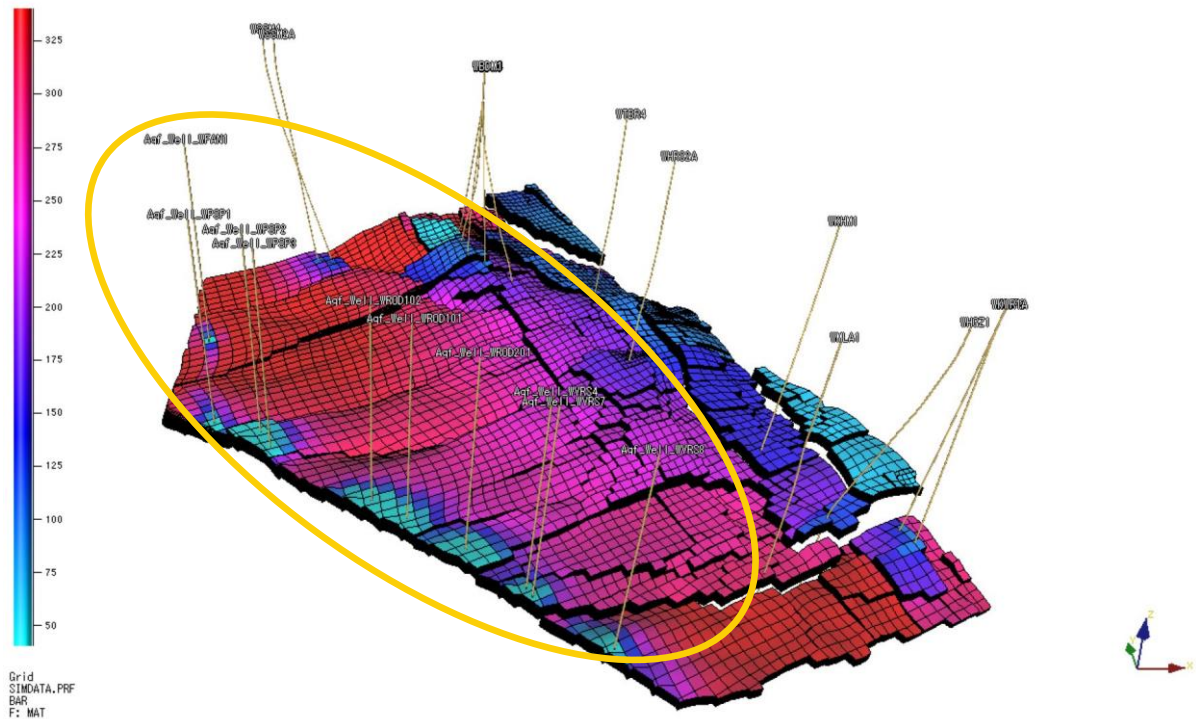


Figure 7: Pseudo-aquifer wells on the southwestern boundary of the Groningen dynamic model.

The pseudo-aquifer wells produce an amount of water that is proportional to the amount of gas produced in the Faan, Pasop, Roden, and Vries fields [1]. Five history-match variables serve as scaling factors to adjust the amount of water produced.

4.2.6 Relative permeability and fluid parameters

The model relative permeabilities are constructed using Corey curves for the various porosity classes. The water and gas end-point relative permeabilities and Corey exponents are input variables that can be used in the history-match. Varying them within the uncertainty ranges previously defined [3] has little impact on the overall history-match. These variables were varied in initial sensitivity studies but set to V6 values for the V7 model calibration runs. The V6 model also used the same optimal values as the V5 model. The V5 model report [3] describes the analysis of relative permeability data and chosen model parameter uncertainties in detail.

Water and gas densities are input variables used to construct the capillary pressure curves. Their values have been left unchanged compared to V6. The V6 model report [1] describes the capillary pressure curves for the Rotliegend and Carboniferous, the latter based on a Carboniferous saturation-height function proposed in 2007 based on Den Velde data [4]. The V7 model uses the same capillary pressure curves as V6. The Groningen PVT models are described in the 2015 (V2.5) model report [2] and are still used.

4.2.7 Gas-in-aquifer properties

The V6 model introduced gas-in-aquifer in the Slochteren formation. The reader is referred to the V6 model report [1] for an extensive description of the evidence for gas-in-aquifer and the model implementation. The input variables for the gas-in-aquifer are:

- *SGR_aqf*: residual gas saturation below the GWC
- *Ng_PRG*: gas Corey exponent applicable to the gas-in-aquifer zone
- *Paleo_contact*: the depth down to which gas-in-aquifer is applied

The paleo contact depth has been introduced in model V7. The gas-in-aquifer is applied to this depth rather than all the way to the bottom of the Rotliegend as in model V6. Implementation of this paleo contact depth was one of the V6 model recommendations and is discussed in Section 5.1.2.

4.2.8 Regional Free Water Levels

Figure 8 shows the 12 initialisation regions within the Groningen field for which Free Water Levels (FWLs) can be set using input variables. The same uncertainty ranges have been used for these FWLs as in the V6 model update⁴. Final values for the regional FWLs are compared to those of V6 in the table in Appendix B. For most regions they are the same as in model V6. Only for the Central region the FWL has been lowered towards the deeper end of the uncertainty range.

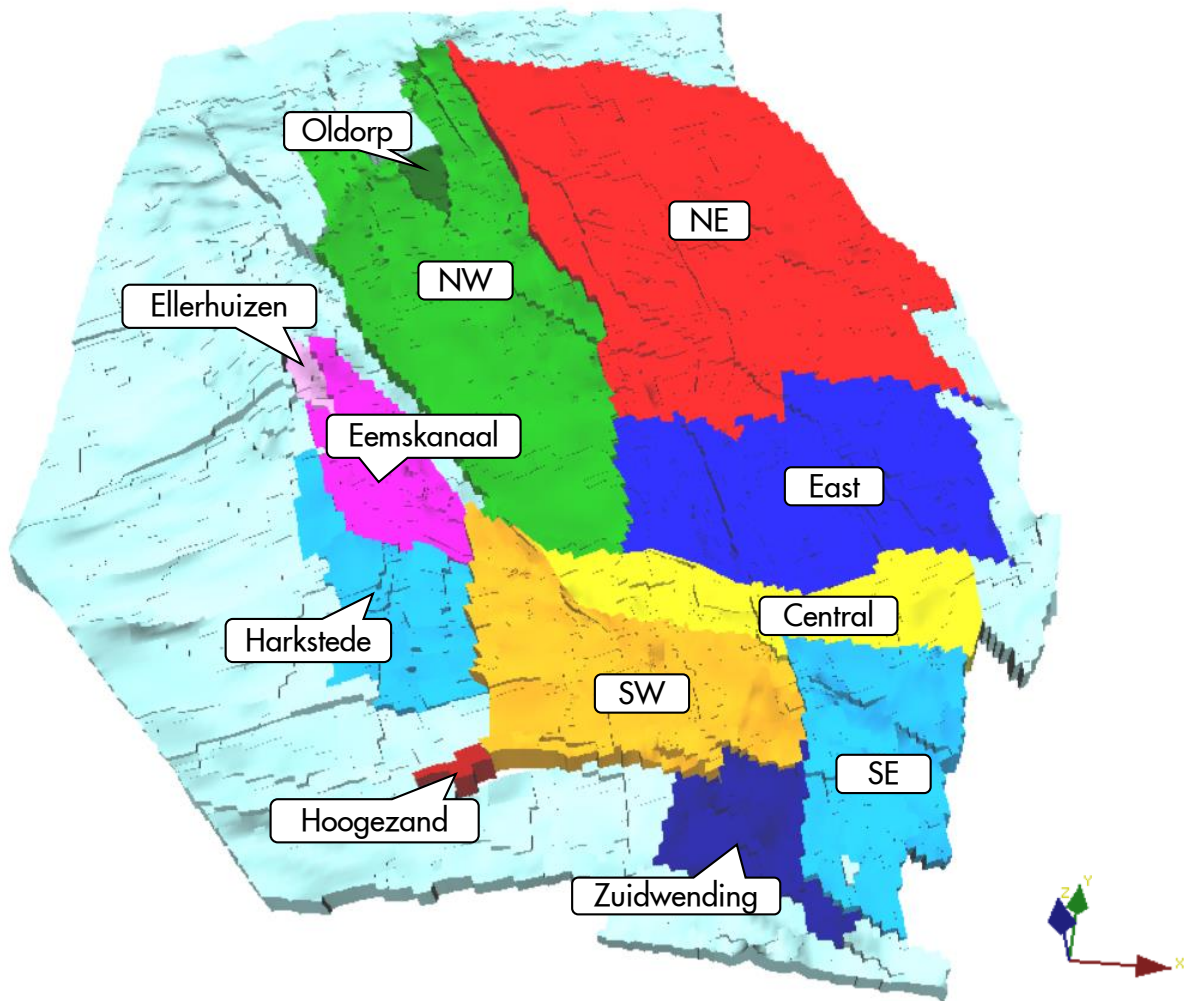


Figure 8: Initialisation regions within the Groningen field. Each region has its own Free Water Level.

The other gas fields that are part of the Groningen model are initialised with their own Free Water Levels that are not part of the history-match input variables. Their values have been documented in the 2015 model report [2].

⁴ Compared to previously reported ranges [2] the maximum depth of *FWL_Gron_Zuidwending* was reduced from 3028 to 3017 m TVDSS in the V6 model history-match.

4.2.9 Rock compressibility

From laboratory tests on Rotliegend core-plugs the following relationship between uniaxial compressibility C_m and porosity has been derived [5]:

$$C_m = 273 \cdot \phi^3 + 68.72 \cdot \phi^2 + 9.85 \cdot \phi + 0.21 \quad [10^{-5} \text{bar}^{-1}] \quad [\text{Eq. 3}]$$

This updated equation has been scripted in the V7 model⁵ and is used directly (without multiplier) to calculate strain in the Rotliegend for ZRP-3, measured late in the Groningen field life (2016-2021). The subsidence occurred over a long period (1972-2018). To match the data with the simplified linear subsidence proxy model built in MoReS (described in the 2015 model report [2]) requires a downward adjustment of the rock compressibility. Like in model V6, this is done through the rock compressibility multiplier (*Compress_rock_mult*). A similar separation between compressibility used for strain in ZRP-3A and subsidence matching has been introduced for the Carboniferous.

4.3 Response variables

The response variables are measures describing the mismatch between the model predictions and the various types of measured data. The history-match workflow aims to minimize these mismatch functions.

The following data sets are used in the history-match:

- Static down-hole pressure measurements (SPG) – up to May-2022
- Repeat Formation Test pressures (RFT), including FIT (Formation Integrity Test) data
- Closed-in tubing-head pressures converted to bottom-hole pressures (CITHP2CIBHP) – up to May-2022
- Long Term Memory Gauge (LTMG) pressure data for Loppersum clusters (LRM, OVS, PAU, ZND) – from end-2018 to May-2022
- Gas-water contact interpreted from pulsed neutron logs (PNL) – up to 2020
- Subsidence data from comparison of 2 levelling surveys (1972 and 2018)
- Strain data from the ZRP-3A DSS cable (cumulative strain with respect to May-2016 after 1, 2, 3, 4, and 5 years)
- Time-lapse gravity data (1996 and 2015, compared to 1978)

The sections below briefly describe these datasets and the corresponding response variables.

4.3.1 SPG RMSE

The SPG data set has been extended to May-2022. Long-term memory gauge (LTMG) data are added to the updated SPG data set: the recorded downhole pressures (in LRM-7, OVS-5, PAU-2, and ZND-3) are converted to datum level, and one data point per quarter is used in the history-match.

The field-wide model mismatch compared to SPG data is quantified by the Root Mean Square Error (RMSE) between model and measurements. Certain locations and certain data periods are much more data dense than others. Since we aim to achieve a good pressure match across the entire field and to early as well as late data, non-equal weighting of data points is required. In addition, the quality of the SPG data is considered.

The 2015 model report [2] describes the following calculation to determine the RMSE with respect to the SPG data for each location j :

⁵ Note that the MoReS model uses pore compressibility as input, approximated as: $CR = \frac{C_m}{\phi}$

$$RMSE_SPG_j = \sqrt{\frac{\sum_{i=1}^{N_j} (p_{m,i} - p_{d,i})^2 w_i}{\sum_{i=1}^{N_j} w_i}}, \quad [\text{Eq. 4}]$$

where N_j is the number of data points for location j , p_m the model pressure, p_d the measured pressure and w_i a weight factor corresponding to the quality of the SPG data point with index i . The quality weight factors have values between 1 and 10. In 2019, a review of the SPG data was conducted and quality scores applied in a consistent manner based on a set of rules. Most of the recent SPG data points are of the highest quality ($w = 10$) unless a high liquid level was found in the wellbore complicating the interpretation.

The 2015 model report further describes that the total model SPG RMSE is a simple average of the location RMSE's:

$$RMSE_SPG_{Field} = \frac{1}{N} \sum_{j=1}^N RMSE_SPG_j, \quad [\text{Eq. 5}]$$

with N the total number of locations. A location corresponds to either a Groningen production cluster, an observation well, injection location (Borgsweer), or a non-Groningen field included in the model.

In practice, the above equations had been implemented differently. Equation 4 is applied not on all the data points at once, but for each 10-year period. Similarly, Equation 5 is applied for each decade, such that a field SPG RMSE is obtained for each decade. The final total SPG RMSE is obtained by averaging these over the six decades between 1963 and 2023. This procedure ensures that data in each period equally weighs into the RMSE that we aim to minimize. Previous Groningen dynamic model updates already used this procedure but overlooked the fact that not all locations have data in each 10-year period. The consequence of this is that a period without data for a particular location yields a location RMSE ($RMSE_SPG_j$) of 0. These zeroes brought down the field average calculated with Equation 5. For model V7, Equation 5 is applied to locations with data only. This means, the number of locations N over which is averaged may vary per decade depending on data availability.

The V6 model report lists an overall SPG RMSE of 1.8 bar [1]. With the updated averaging method, the V6 model SPG RMSE becomes 2.8 bar.

Additional SPG RMSE's are calculated for each Groningen pressure monitoring region, by applying Equation 5 to those locations that fall in the region of interest. The monitoring regions are described in the Groningen surveillance requirements [6] and monitoring strategy documents [7].

4.3.2 RFT RMSE

A repeat formation test (RFT) measures pressure at different depths in the well. This is usually done just after drilling a new well. For each well with RFT data, a local RFT RMSE is calculated as follows:

$$RMSE_RFT_j = \sqrt{\frac{1}{N_j} \sum_{i=1}^{N_j} (p_{m,i} - p_{d,i})^2}, \quad [\text{Eq. 6}]$$

With N_j the total number of RFT pressure data points for well with index j , and p_m and p_d the model and measured pressure data points with index i . Due to the vertical gridding, for some specific data point depths the model interpolates between the pressure in the Ten Boer and pressure in Upper Slochteren, causing an artificially large mismatch with the measurement. These data points have been taken out of the RMSE calculation.

The overall model mismatch to the RFT data is calculated as a simple average of $RMSE_RFT_j$ over all wells that have RFT data. The last RFT data was obtained for ZRP-3A in August 2018. A small number of RFT measurements in the Carboniferous that were not used in the V6 history-match have been incorporated for V7 (see also Section 6.4).

4.3.3 CiTHP2BHP RMSE

The V4 model update [8] introduced the CiTHP2BHP data set. Time-dependent functions are used to convert CiTHP to BHP [9]. The parameters in these functions are obtained by fitting to data (where both CiTHP and BHP are available). For a dozen clusters these parameters have been retuned in 2020. The full set of parameters is given in 0. The CiTHP2BHP data set has been extended to May-2022.

The RMSE with respect to the CiTHP2BHP data is calculated for each cluster. To obtain the total CiTHP2BHP RMSE the cluster RMSE's are averaged⁶.

4.3.4 PNL RMSE

The calculation of the mismatch to the PNL data is described in the 2015 model report [2] but repeated here to explain the difference with previously reported values. For each well with PNL data, a comparison is made between the interpreted GWC depth from the PNL (h_d) and the GWC depth from a pseudo-log generated in the MoReS model (h_m) at the same date. For each well the RMSE is calculated as follows:

$$RMSE_PNL_j = \sqrt{\frac{1}{N_j} \sum_{i=1}^{N_j} (h_{m,i} - h_{d,i})^2}, \quad [\text{Eq. 7}]$$

with N_j the number of data points for well j .

The total PNL RMSE should be calculated by averaging of the local RMSE's over the N locations with data:

$$RMSE_PNL_{Field} = \frac{1}{N} \sum_{j=1}^N RMSE_PNL_j. \quad [\text{Eq. 8}]$$

It was discovered that the script to calculate the PNL RMSE contained an error resulting in much too low values. Instead of Equation 8, the following equation was scripted:

$$RMSE_PNL_{Field} = \frac{1}{N} \sqrt{\sum_{j=1}^N \left(\frac{1}{N_j} \sum_{i=1}^{N_j} (h_{m,i} - h_{d,i})^2 \right)}. \quad [\text{Eq. 9}]$$

In other words:

$$RMSE_PNL_{Field} = \frac{1}{N} \sqrt{\sum_{j=1}^N (MSE_j)}, \quad [\text{Eq. 10}]$$

With MSE indicating the Mean Square Error.

The simple example in Table 4 illustrates the difference between the calculation with Equation 8 versus Equation 9 or 10. It is clear from the example that the "average" obtained with Equation 10 is too low (even lower than the minimum location RMSE in this example). The reported PNL RMSE in the V6 report based on Equation 10 was 2.8 m. Using the correct Equation 8 would have resulted in a total

⁶ The sum of all individual cluster RMSE's is divided by the number of clusters that have CiTHP2BHP data. A few clusters don't have CiTHP2BHP data. These were previously included in the averaging script, leading to smaller total RMSE values.

PNL RMSE of 13.2 m instead. The PNL mismatch has been underreported for models V2.5 [2], V4 [8], V5 [3], and V6 [1].

Table 4: Illustration of incorrect RMSE calculation (in red) for PNL data.

| Location | RMSE | MSE |
|--------------------------|---|-----|
| 1 | 10 | 100 |
| 2 | 8 | 64 |
| 3 | 6 | 36 |
| Average ([Eq. 8]) | 8 | |
| Applying [Eq. 10] | $\frac{1}{3}\sqrt{(100 + 64 + 36)} = 4.7$ | |

For the V7 history-match Equations 7 and 8 are used with one additional step. Certain clusters have multiple wells with PNL data. First the well PNL RMSE's calculated with Equation 7 are averaged per location. Equation 8 is then applied to average over the locations. Only PNL's that show a measured GWC rise over time are included in the comparison. This updated calculation yields a PNL RMSE of 10.4 m for the V6 model.

4.3.5 Subsidence RMSE

Subsidence data from 2018 with respect to 1972 has been obtained from the Geomechanics department on a 500 m by 500 m 2D grid. The data is interpolated to generate subsidence values corresponding to the MoReS grid (top layer). Where no subsidence data is available, positive values are given such that these grid cells can later be filtered out in the comparison.

When the simulation reaches June 2018, MoReS calculates subsidence using the proxy model described in the 2015 (V2.5) model update report [2] based on the model by Geertsma and van Opstal [10]. This calculation uses model grid block pressures and adjusted rock compressibility as described in Section 4.2.9. The subsidence RMSE is calculated as follows:

$$RMSE_Subsidence = \sqrt{\frac{1}{N_s} \sum_{i=1}^{N_s} (S_{m,i} - S_{obs,i})^2}, \quad [\text{Eq. 11}]$$

with N_s the number of grid blocks in the 2D grid with subsidence data, $S_{m,i}$ the proxy model subsidence, and $S_{obs,i}$ the observed subsidence for grid block with index i .

4.3.6 DSS RMSE

ZRP-3A Distributed Strain Sensing (DSS) data was introduced in the V6 model update. The method of processing the raw data to an upscaled data set that can be compared on the dynamic model grid is described in a note by Kole, 2018 [11]. Kole performed similar processing for the data up to May-2021 for comparison on the updated V7 model grid. This resulted in five data sets to compare the observations to calculated values of cumulative strain based on model grid block pressure change and C_m , which is a function of grid block porosity for the Rotliegend (Section 4.2.9 [Eq. 3]). Cumulative strain for each set is taken in comparison to May-2016, because from this date the signal is undisturbed [11].

For each of the five data sets the RMSE between calculated and observed strain data points is calculated. The total reported DSS RMSE is the average of these five values.

4.3.7 Gravity RMSE

In 2017, comparison to two time-lapse gravity data sets (1996 and 2015, both compared to 1978) was built in MoReS. The data, model implementation, and analysis are extensively described in the report by van Oeveren (2017) [12]. The same gravity data sets and methodology are still used.

Since the gravity data carries a relatively large uncertainty, the RMSE is calculated not with respect to the measured value, but including uncertainty [12]:

$$RMSE_Gravity = \sqrt{\frac{\sum_{s=1}^{N_s} (\Delta g_{s,m} - (\Delta g_{s,d} \pm \sigma_s))^2}{N_s}}, \quad [\text{Eq. 12}]$$

where $\Delta g_{s,d}$ is the gravity change measured at station s , $\Delta g_{s,m}$ the calculated model gravity change at station s , σ_s the estimated error on the measurement at station s , and N_s the total number of stations for which reliable data is available. The gravity RMSE is calculated for all stations plus separately for those above the Carboniferous.

A small update has been made to the calculation script to make the Gravity RMSE consistent with Equation 12. For comparison, the gravity RMSE for the V6 model has been recalculated as well. The corrected V6 total gravity RMSE is 5.0 μGal instead of the 4.8 μGal reported in the V6 model report [1].

4.4 History-Match process

The following steps have been used to obtain a global history-match:

1. Simulate a set of runs based on a space-filling experimental design for k input variables with low-base-high value ranges (and uniform distributions).
2. Analyse simulation results in Autosum:
 - a. Response modelling (using machine learning algorithms)
 - b. Input variable importance for the various responses
 - c. Visualise response-feature relationships
3. Decide which input variables are used in the next simulation cycle and adjust low-base-high value ranges if necessary.
4. Steps 1-3 are repeated until the best field wide SPG match doesn't significantly improve anymore in subsequent cycles.
5. Out of models with a similarly good match to SPG data select model with best match to other data (subsidence, PNL, RFT, CITHP2BHP).

Further dedicated cycles have been carried out to:

- Assess effect of extending gas-in-aquifer area to Southwest periphery
- Improve the pressure match in specific regions
- Improve the match to specific data sets
- Calibrate the Carboniferous properties

More than 15,000 simulations have been run in total, as part of 25 experimental designs and additional sensitivities.

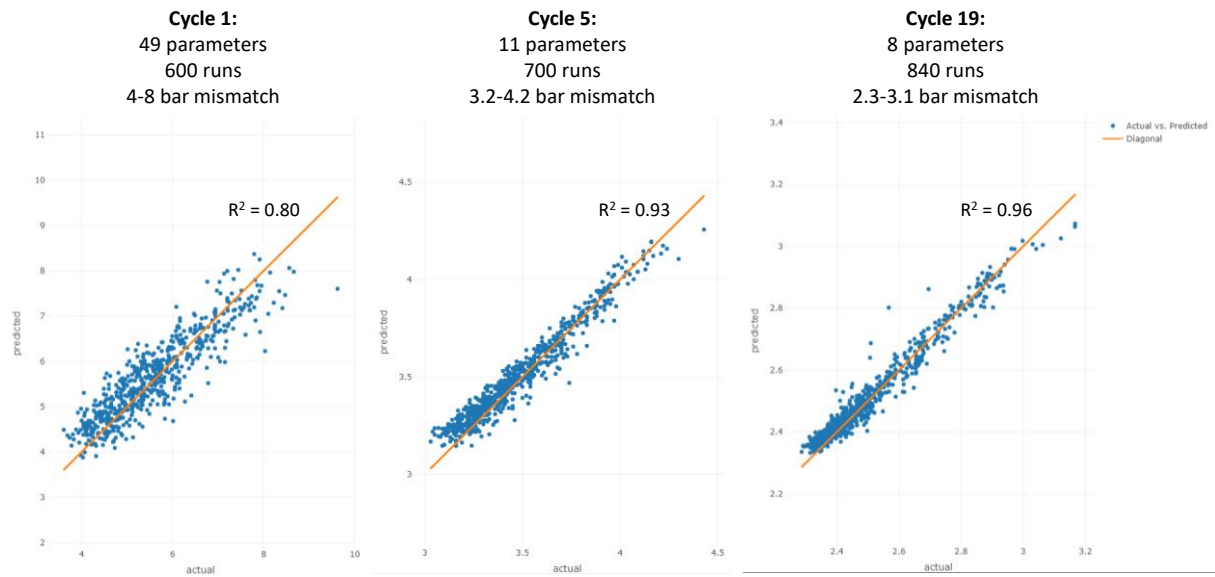


Figure 9: Evolution of the model wide SPG RMSE over the history-matching cycles. The plots show predicted SPG RMSE of a machine learning model versus actual SPG RMSE from simulation, for blind tests (data not used to train the machine learning model).

Figure 9 shows the evolution of the model-wide SPG RMSE over the history-matching cycles. In the first cycle, the SPG RMSE for the bulk of the runs ranged from 4 to 8 bar. This experimental design was based on 49 input variables. Later designs used a lower number of features, focusing on those with most impact on the model wide SPG match (and setting other input variables to more-or-less optimal values determined from previous cycles). The plots in Figure 9 show a cross-validation of predicted SPG RMSE against actual SPG RMSE, where the prediction is from a machine learning model (trained with simulation data) and actual as determined from simulation. The ML model prediction improves as the number of data points (simulation runs) increases compared to the number of features (input variables). In Cycle 19, the best simulation runs had an SPG RMSE of about 2.3 bar.

5 Model Adjustments and New Features

This chapter discusses adjustments made to model V7 to improve the history-match in specific regions. The implementation of the paleo contact for gas-in-aquifer is discussed in Section 5.1.2 as part of the discussion of Kolham and the Southwest periphery. The improvement of the Bedum history-match is described in Section 5.2. Section 5.3 describes adjustments in the Northeast of the model, and Section 5.4 introduces a new feature that improves both the Borgsweer pressure match and the match to the observed GWC rise in DZL-1 from PNL data.

5.1 Kolham and Southwest periphery

5.1.1 Variables impacting Kolham pressure match

One of the main areas that needed improvement of the V6 history-match is the Kolham area, highlighted in the right plot of Figure 10. The model pressure in KHM-1 matches the measured data reasonably well up to 2010 but deviates more and more for the more recent data (left plot of Figure 10). The V6 model datum pressure is 12 bar lower than measured in January 2020.

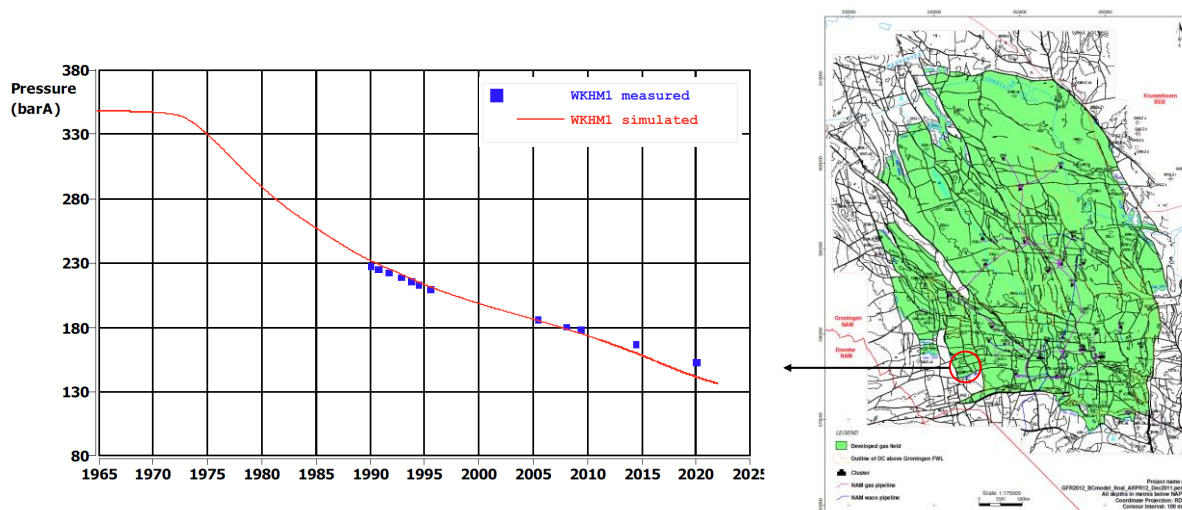


Figure 10: V6 Model pressure history-match in KHM-1. The Kolham area is highlighted in red in the map on the left.

Two input variables have historically been used to control the pressure history-match in KHM-1 [8]: *Kolham_gbv_mult* and *LogFaultSeal_KHMTrough_WE*. The first is a GBV multiplier for the Kolham fault blocks. The second controls the transmissibility of the fault separating Eemskanaal and Kolham (Fault M28 in Figure 11). The Kolham blocks deplete solely through this connection with the Eemskanaal area. Adjusting the transmissibility of fault B60 (Figure 11) using the variable *LogFaultSeal_EKLW* has no impact on the Kolham pressure match, due to the large throw of this fault where it borders the Kolham blocks (no reservoir juxtaposition).

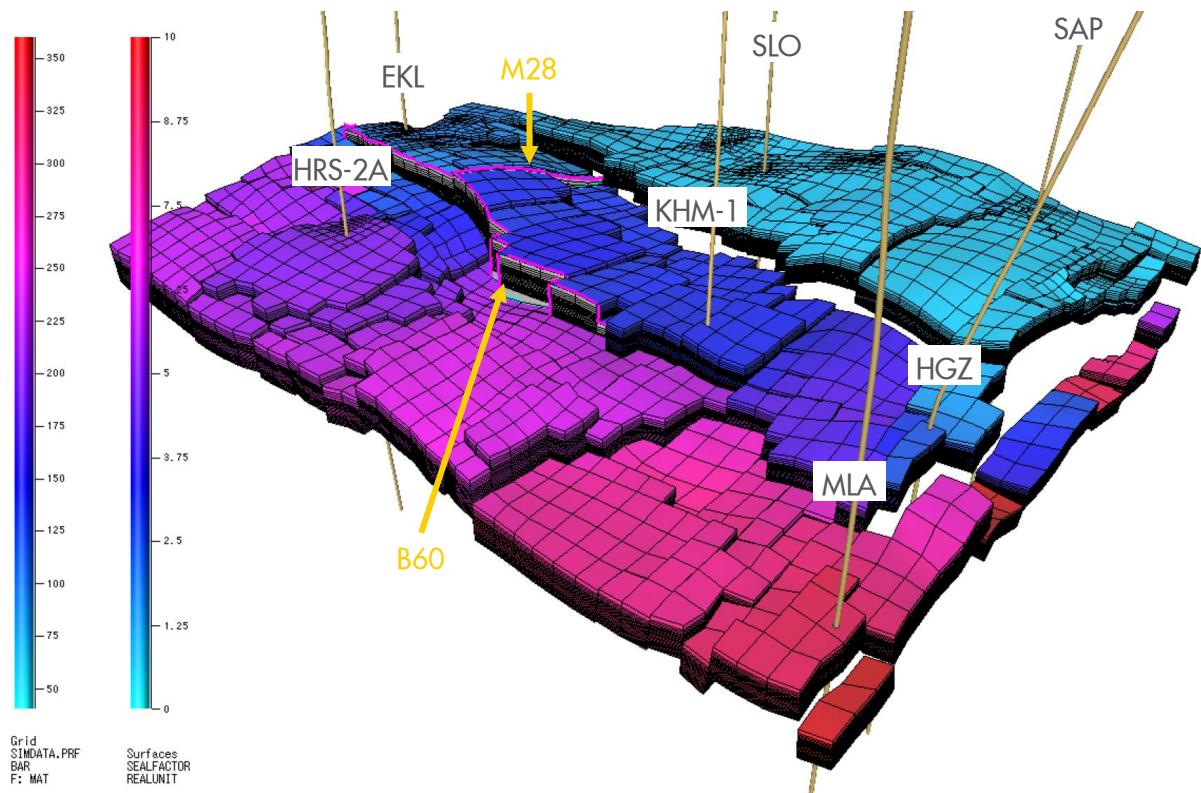


Figure 11: Simulated pressure (on 1-5-2022) in 3D model view around Kolham area. Only ROSL layers are shown.

Figure 12 shows the initial gas saturation in the Kolham area. Parts of the Southern Lauwerszee aquifer surround the Kolham area to the South and East. However, the aquifer is poorly connected to Kolham due to very limited juxtaposition windows, as illustrated in the model view in Figure 13.

Adjusting the Kolham GIIP (through its GBV multiplier) and/or the M28 fault transmissibility shifts the model pressure curve up or down. However, when the pressure in KHM-1 is matched for the earlier data, it is always under-estimated for the later data. And vice versa, when the pressure is matched for the later data, it is over-estimated for the earlier data. Kolham needs a mechanism that provides some slow (late) pressure support or that decreases depletion in later stages (post-2008).

Since there are more data points in the 1990's than in the last 10 years, a special response variable is introduced for the Kolham pressure history-match based on equal weighting of the data for each of 4 periods illustrated in Figure 14. This prevents the history-match to be dominated by the early data.

Several attempts were made to try to improve the connection between Kolham and the Southern Lauwerszee aquifer. Figure 15 and Figure 16 show that the aquifer compartments neighbouring KHM-1 have a significantly higher pressure. Fault M9 (Figure 15) is fully open (no seal factor is applied). The same is true for fault B52a shown in Figure 16. Artificially increasing the transmissibility of Fault B52a by a factor 100, reduces the pressure difference across this fault from 20 to 2 bar. The resulting pressure increase in KHM-1 however is only 0.1 bar.

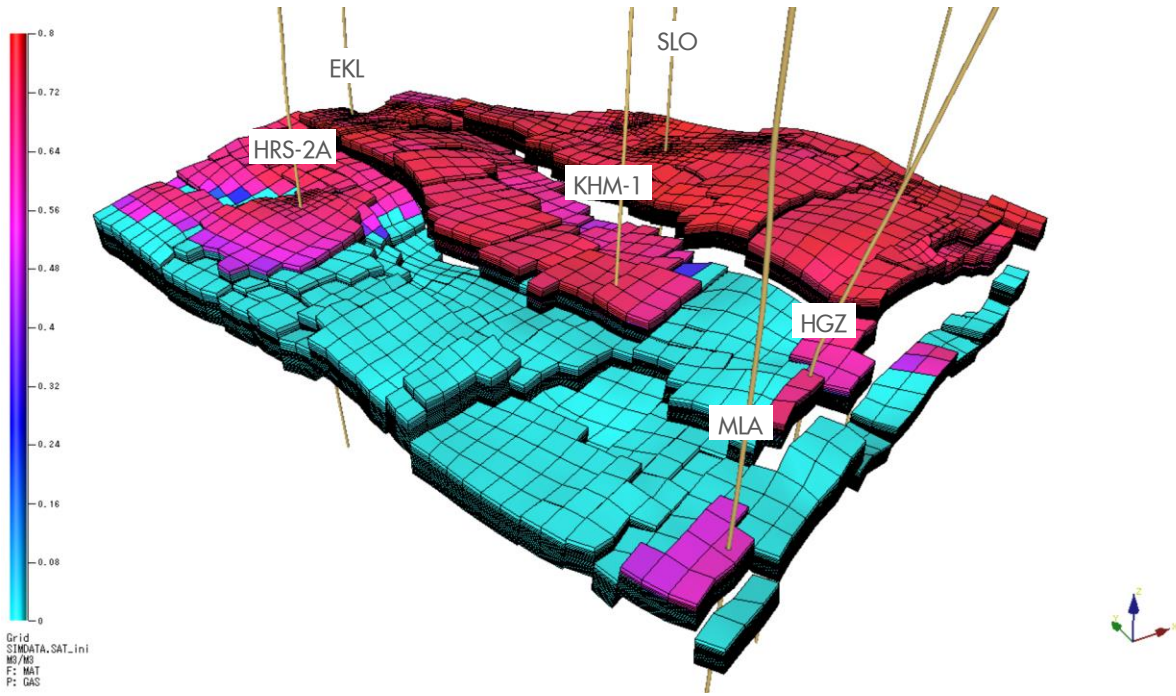


Figure 12: Initial gas saturation in 3D model view around Kolham area. Only ROSL layers are shown.

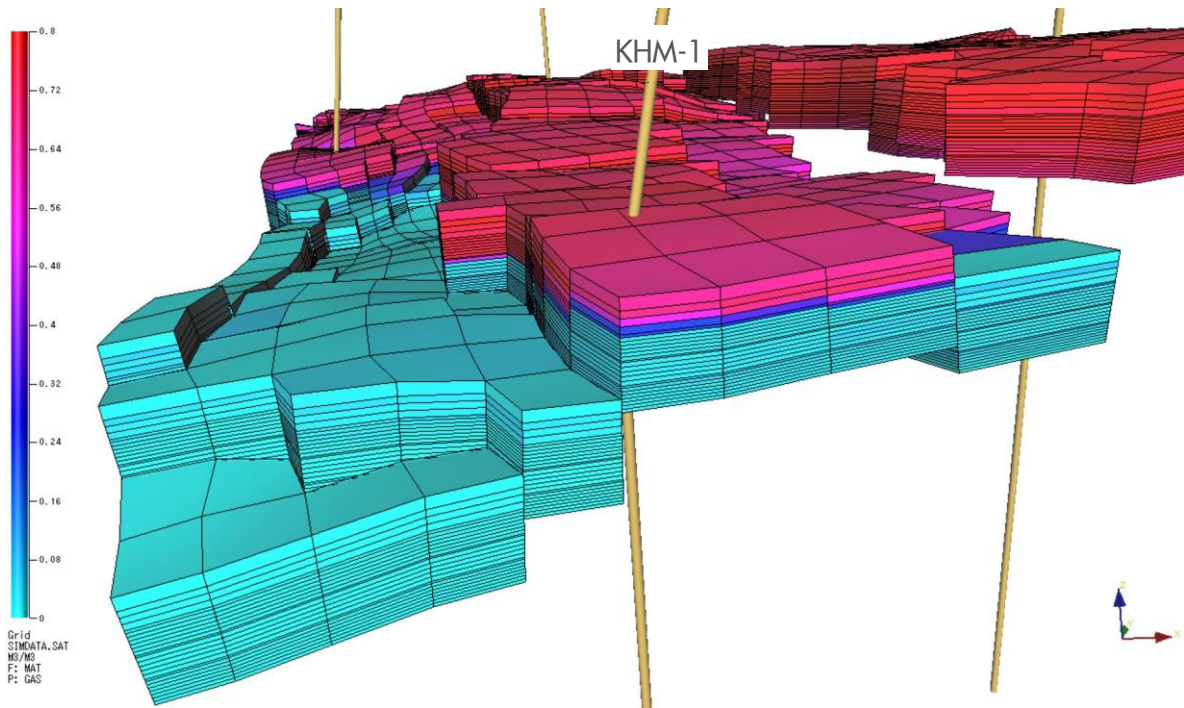


Figure 13: Model cross section looking at KHM-1 from the South. Shown is simulated gas saturation on 1-5-2022 in ROSL layers.

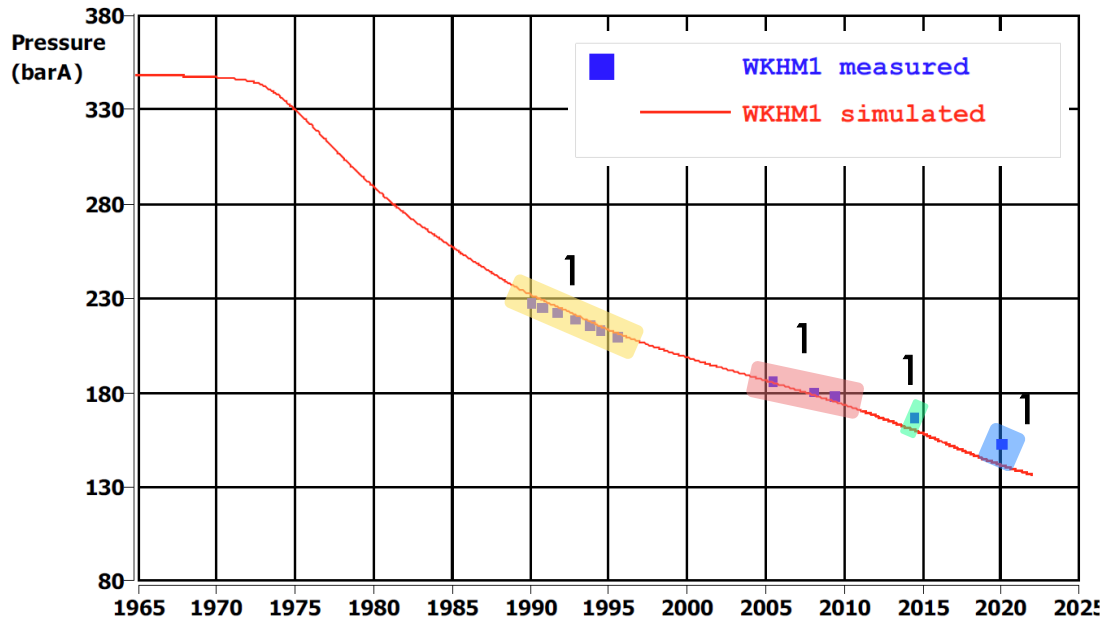


Figure 14: Division of measured pressure data in KHM-1 in four time periods for equal weighting in RMSE_KHM_SPG_adj.

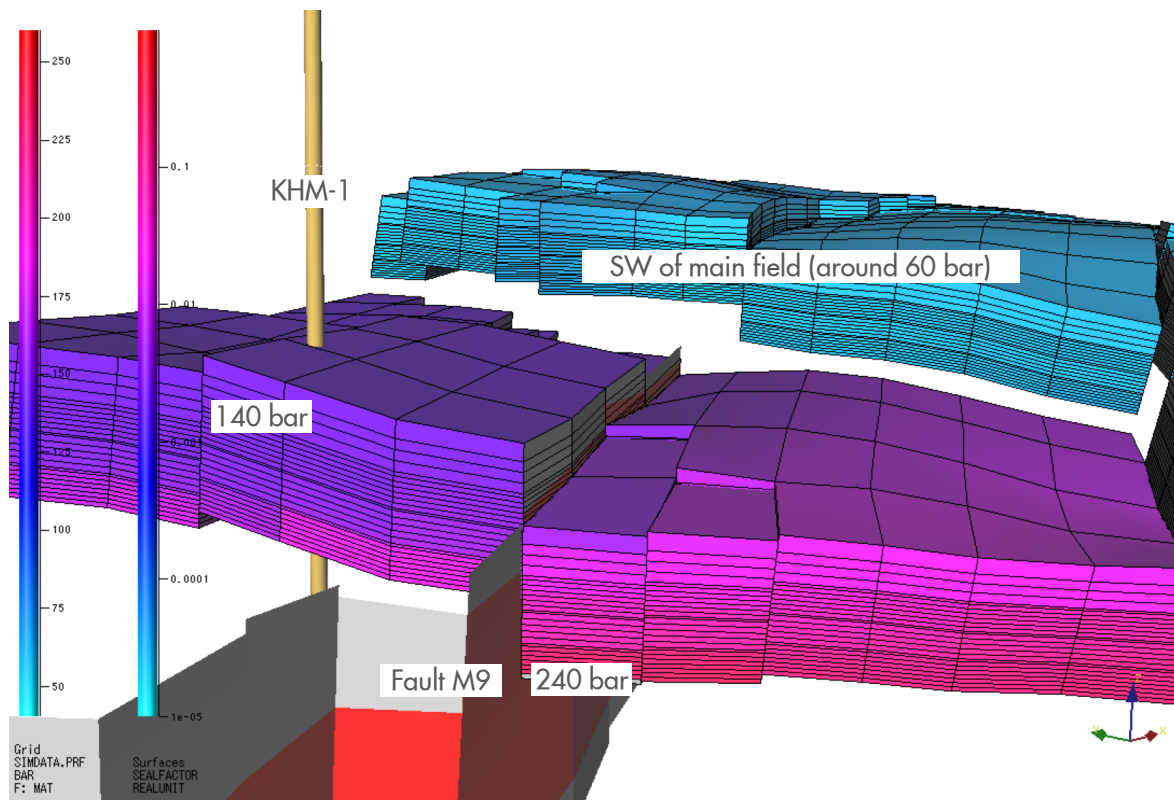


Figure 15: Connection between KHM-1 and Southern Lauwerszee aquifer to its South.

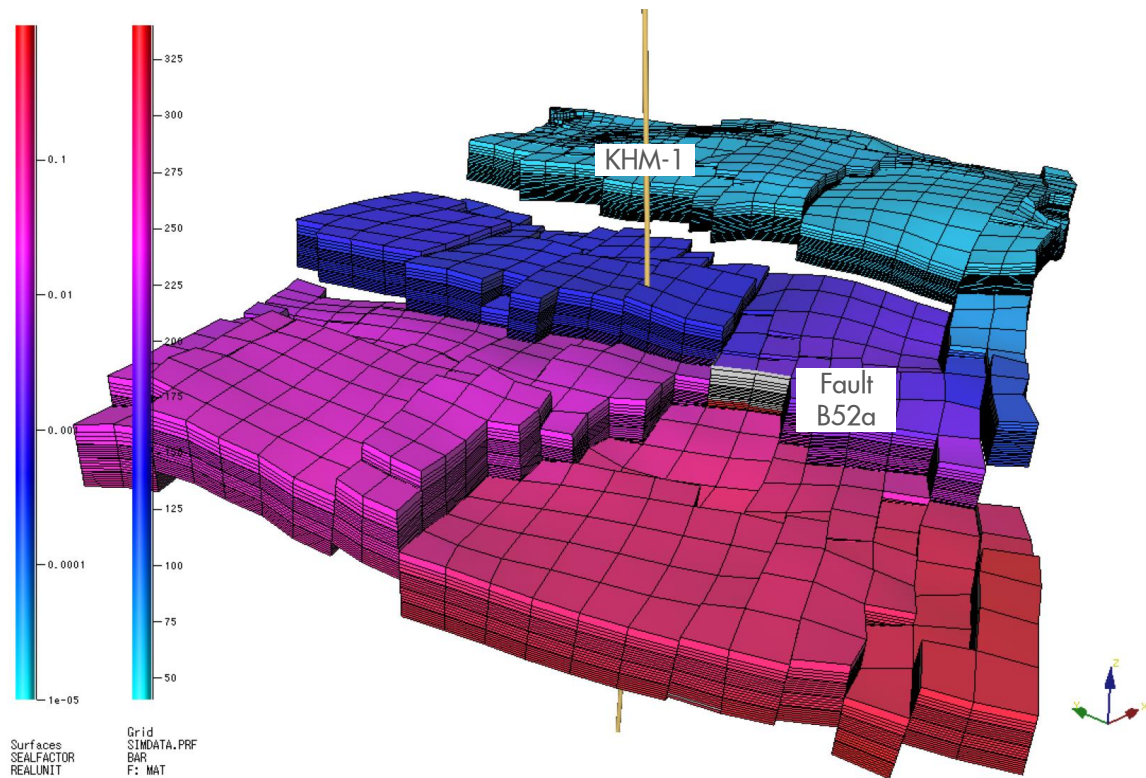


Figure 16: Fault B52a in the Southern Lauwerszee aquifer.

Turning off the pseudo-aquifer wells that deplete the Southern Lauwerszee aquifer has no impact on the Kolham pressure, where it does impact the pressure in other areas like Warffum and Midlaren. Similarly, boosting the aquifer permeability in the area has more impact on other areas than on Kolham. Based on the current model it doesn't seem possible to significantly affect the Kolham pressure match by adjusting the properties of the neighbouring aquifer.

5.1.2 Gas-in-aquifer extension and Paleo contact

The area in which gas-in-aquifer is present in the Slochteren reservoir excluded Kolham and the South-West periphery in model V6. The reason for this is that in this area there is a lack of supporting data compared to in the North part of the field. Figure 17 shows the direct evidence from PNx and OH logs across the field. The KHM-1 open hole log was interpreted to have residual gas below the GWC (Figure 17, right). The interpretation of DHI data in the Kolham area was interpreted as having no gas-in-aquifer, but this was a low confidence interpretation. Other assessments in 2018 were based on indirect data. At the time, an assessment was made whether the match to PNL, RFT, and subsidence data improved if gas-in-aquifer was included or not. Since the history-match depends on so many variables this is not considered strong evidence. It was found that including gas-in-aquifer in the SW part of the model did not improve the history-match. But for this comparison gas-in-aquifer was implemented all the way down to the bottom of the Slochteren aquifer, and not limited to a certain depth. In the V7 model, a "Paleo contact" has been introduced as per V6 model recommendations [1]. In one of the early history-match cycles an experimental design of 1000 runs was simulated with and without extension of the PRG area to the South-West, based on an estimated paleo contact depth of 3158 m. Including PRG in the South-West resulted in a slightly improved pressure match in the South-West periphery, and an improved overall match to PNL data. Therefore, it was decided to include PRG in the South-West for subsequent history-match cycles.

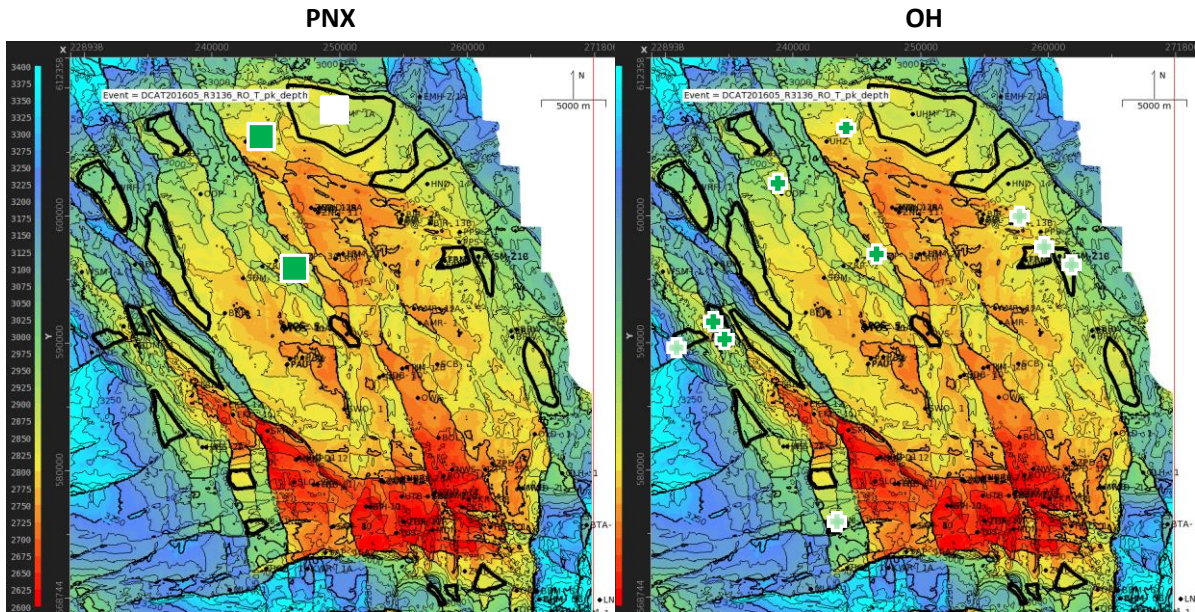


Figure 17: Evidence for paleo residual gas (PRG) from PNX and OH logs. Green symbols indicate evidence in favour of PRG, with darker colours indicating higher confidence levels. The white square denotes inconclusive evidence from the UHM-1A PNX.

Figure 18 compares the extent of gas-in-aquifer in the V6 and V7 models. The PRG area in V6 excludes the South-West of the model but has gas-in-aquifer all the way down to the bottom of the Lower Slochteren.

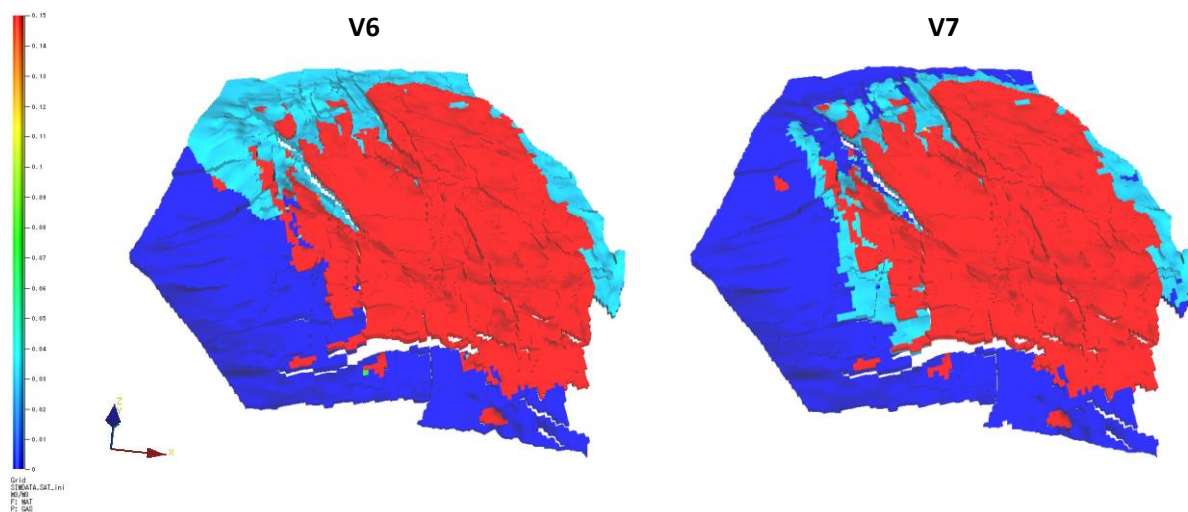


Figure 18: Implementation of gas-in-aquifer in the V6 and V7 models. Shown is initial gas saturation in the Slochteren (model layers 4-34).

The right of Figure 18 shows the V7 implementation using a paleo contact depth of 3158 m TVDSS. As there is uncertainty around this depth it is introduced as a new history-match variable. Because the gas-in-aquifer is limited to the paleo contact depth, only a limited part of the Southern Lauwerszee aquifer is affected.

5.1.3 Kolham history-match

Inclusion of residual gas-in-aquifer in the Kolham area increases the late pressure in KHM-1 compared to the early pressure slightly. The effect is in the right direction but not significant. The only remaining pragmatic option to improve the KHM-1 history match is to introduce a time dependent fault

transmissibility. To decrease the late-time Kolham depletion the M28 fault needs to become less transmissible over time. This has been implemented by changing (*LogFaultSeal_KHMTrough_WE*) by *Delta_KHMTrough_WE* between 2006 and 2015 in a few steps. It turns out a *Delta_KHMTrough_WE* of -0.36 is required for a good history-match. This means that the fault transmissibility reduces from 0.0059 (prior to 2006) to 0.0026 (after 2015). This is a relatively modest change from a largely sealing fault to an even more sealing fault.

Adjusting the fault is the most pragmatic way to match the data. Suggesting a mechanism to explain the fault transmissibility change, e.g., related to pressure reduction, saturation changes, compaction, or possibly seismic events would be speculation. Implementing the change in several small steps works better than a single sudden change. An alternative explanation for the KHM-1 pressure behaviour is that there is some form of slow pressure support missing in the model, for example the aquifer connection not being represented accurately in the static model. Though the precise mechanism is unknown, the pragmatic solution results in a good match to all KHM-1 pressure data (Figure 19). This way we avoid a mismatch in the recent pressure distribution that would work its way through into subsidence and seismic risk predictions.

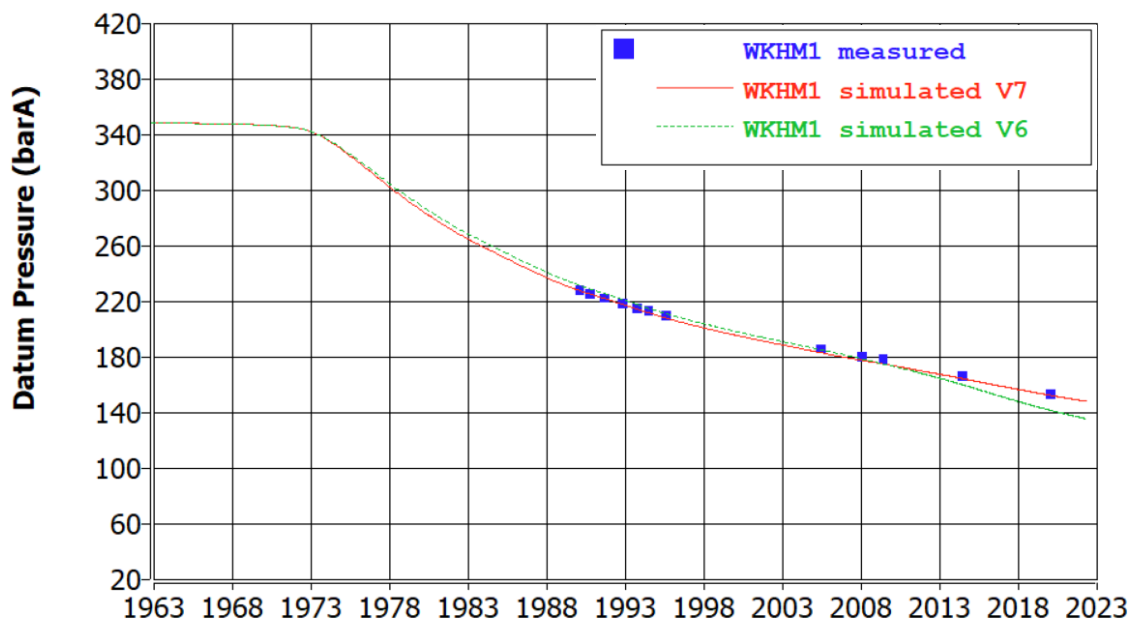


Figure 19: Improvement of KHM-1 pressure history-match.

5.2 Bedum

One of the V6 model report recommendations was to improve the BDM-5 pressure match [1]. BDM-5 is the most southern well in the Bedum field. The modelling of the Ten Boer layers in Petrel has been corrected in this area (Section 3.2). However, this had little impact on the BDM-5 pressure match. For the entire Bedum area, a single GBV multiplier of 0.866 was used in model V6. This resulted in a GIIP of 4.0 NBcm for the Bedum South blocks. This is much higher than expected based on the Bedum RCCN GIIP range (Table 5). As a result, there is not enough pressure depletion in BDM-5 in model V6.

Separate GBV multipliers have been introduced for the Bedum and Bedum South segments in model V7. The GIIP for both Bedum and Bedum South in model V7 is now close to the base case estimate.

Table 5: Comparison of Bedum GIIP estimates to Bedum GIIP in Groningen models.

| | Bedum GIIP estimate (NBcm) | | | GIIP in Groningen model (NBcm) | |
|-------------------------|----------------------------|------|------|--------------------------------|------|
| | Low | Base | High | V6 | V7 |
| Bedum (excluding South) | 10.2 | 12.1 | 14.2 | 14.9 | 11.5 |
| Bedum South | 1.9 | 2.3 | 2.8 | 4.0 | 2.4 |
| Total | 12.2 | 14.4 | 17.0 | 18.9 | 14.2 |

There are many fault seal factors in the Bedum region that can be set in the dynamic model. These have been calibrated in dedicated history-match cycles. Figure 20 shows the improvement in the BDM-5 history-match that was achieved in the final V7 model. The Bedum field SPG RMSE improved from 15.3 bar for model V6 to 8.9 bar in V7.

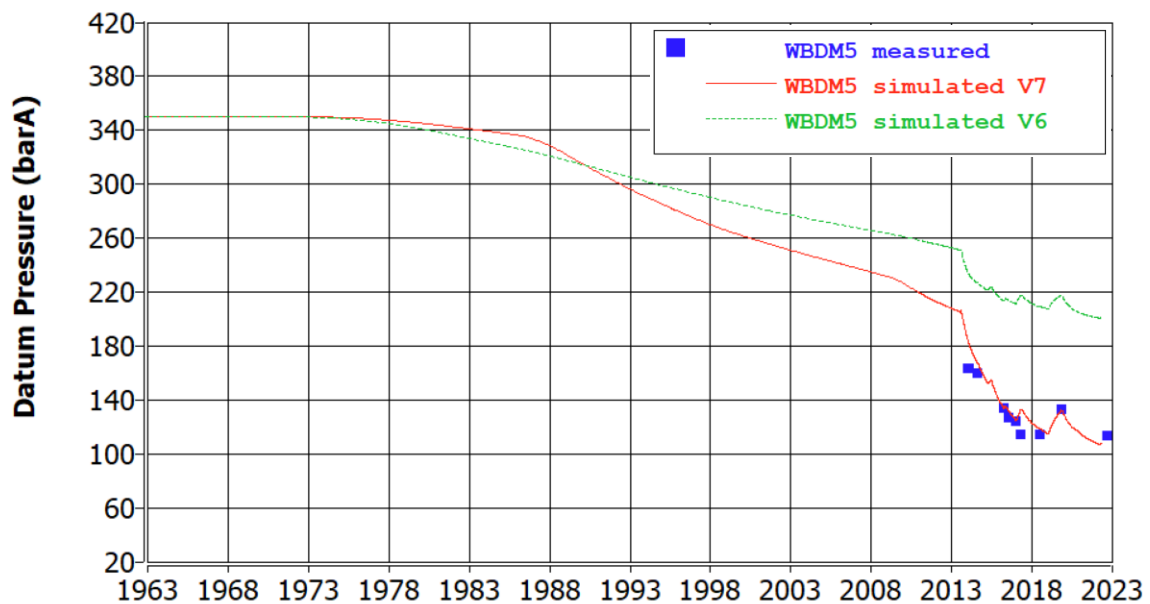


Figure 20: Improvement of BDM-5 pressure history-match.

5.3 Region North-East

The 1978 UHZ-1 RFT shows 35 bar differential depletion between the Upper and Lower Slochteren. According to Vos [13] this is likely caused by pressure differentials across the Ameland shale or across some continuous shales in the Lower Slochteren. The pressure differential in the UHZ-1 RFT is not matched in the V6 model. The dynamic model applies a reduction to the vertical permeability of the Ameland shale in the northern part of the field. In V6, this permeability multiplier was applied only where the Ameland layer had a minimum thickness of 7.5 m. The idea behind this is that a thinner Ameland shale is less likely to be laterally continuous and therefore vertically sealing. Figure 21 shows that the 7.5 m thickness threshold results in the exclusion of the UHZ-1 region from an otherwise continuous area in the North in which the Ameland vertical permeability multiplier is applied. This does not make sense based on the UHZ-1 RFT data.

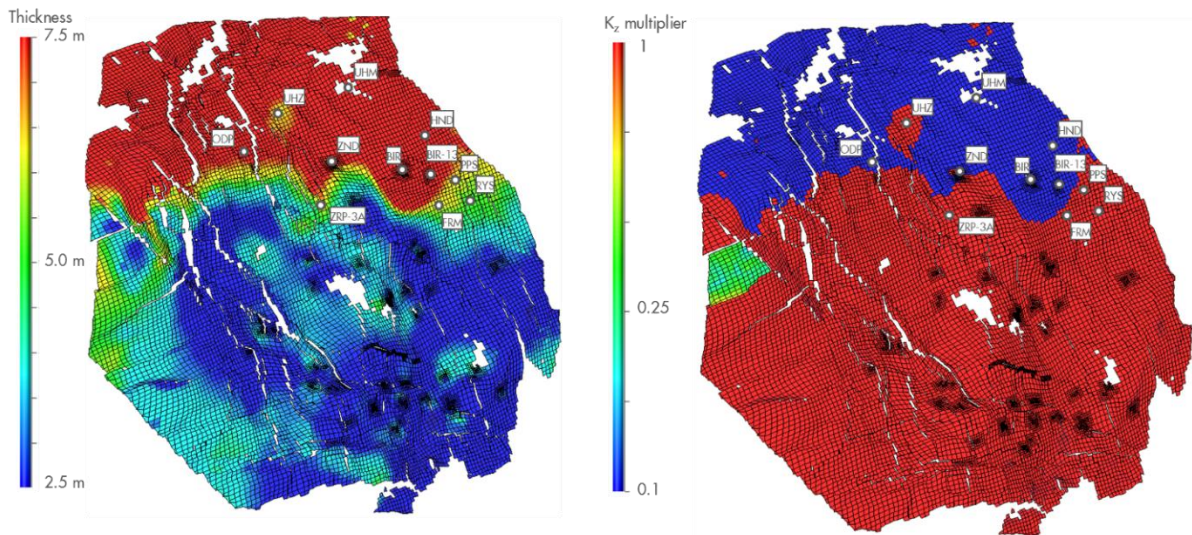


Figure 21: Map of Ameland shale thickness (left) and vertical permeability multiplier (right) in model V6 (Figure 8-4 in [1]).

In model V7, the Ameland thickness threshold is reduced to 6.4 m such that the UHZ-1 region is included, and the multiplier is applied in a more continuous area. This modification by itself is not enough to match the UHZ-1 RFT data. In addition, the transmissibility of the Lower Slochteren needs to be reduced in the area.

To obtain a history-match, the Rotliegend permeability is boosted in all Groningen regions. The regional log-permeability multipliers in V6 as well as V7 are close to 1, which means the permeability is adjusted to be close to the P10 values. The permeability multiplier is porosity-dependent, as explained in Section 4.2.2. For the North-East region, the absolute permeability multiplier ranges from about 1.5 for high porosities to 8 for the lowest porosities. A reduction of permeability by a factor 8 in the Lower Slochteren is required to match the UHZ-1 RFT behavior. This means that low porosity grid blocks are more or less set back to their original permeability. This new multiplier (*Delta_k_North_ROSL*) is applied in model region "ProductionRegion_North" which corresponds to the region outlined in Figure 22.

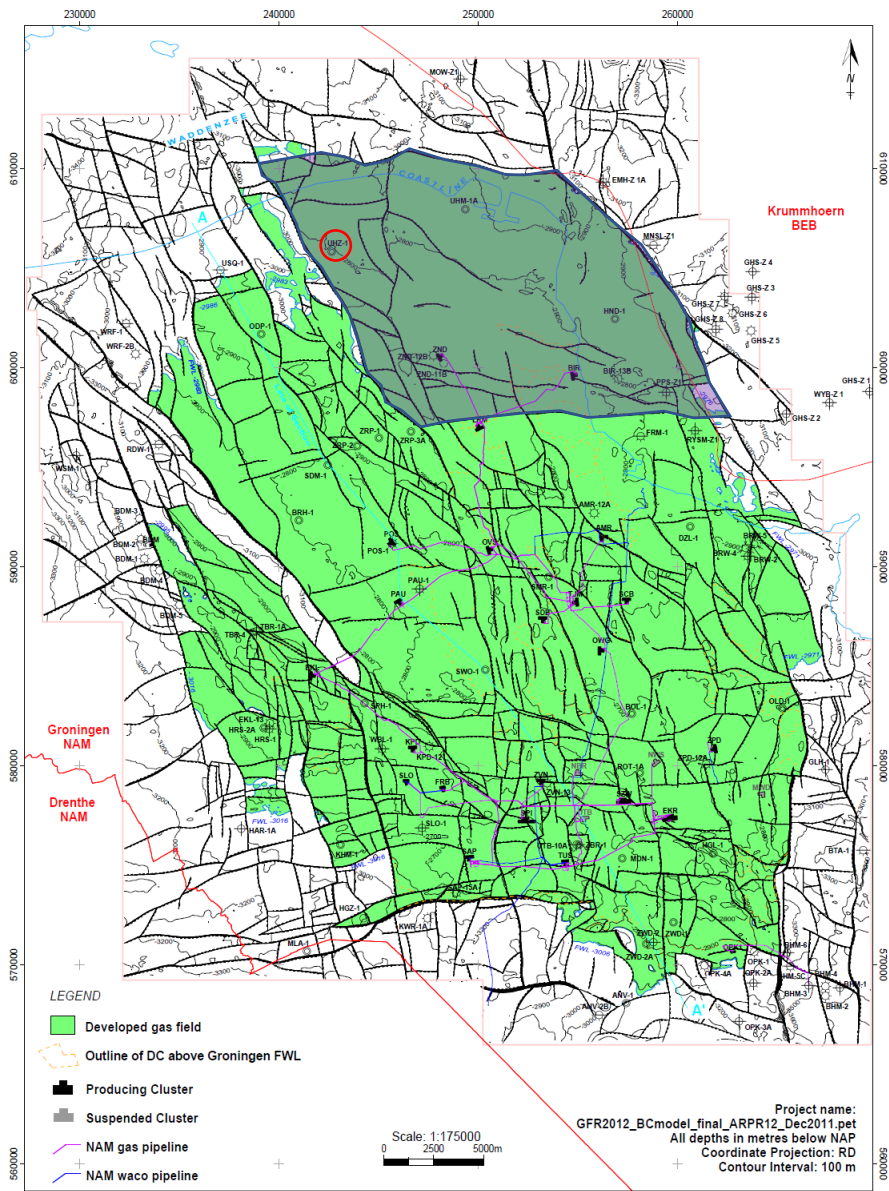


Figure 22: Groningen field map (top Rotliegend) with model region ProductionRegion_North and UHZ-1 highlighted.

Figure 23 compares the V7 and V6 model history-match of the UHZ-1 RFT. The V7 model matches the pressure in both Upper and Lower Slochteren. The overall regional pressure history-match has improved as well. The RMSE for the SPG data in region North-East has improved from 1.7 bar in V6 to 1.2 bar in V7. This includes data from clusters Bierum, 't Zandt, Leermens, and observation wells HND-1, UHZ-1, and UHM-1A.

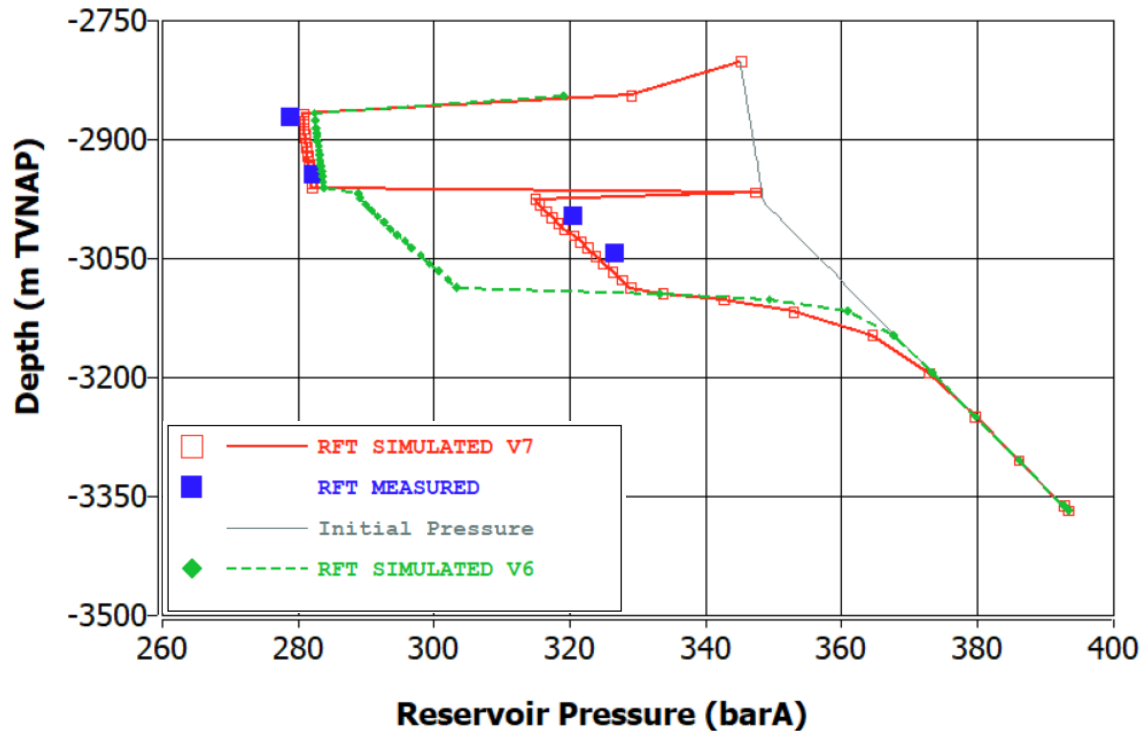


Figure 23: Improved history-match of UHZ-1 RFT (02-09-1978).

5.4 Borgsweer and DZL-1

In an attempt to improve the Borgsweer pressure history-match a dilemma was encountered. A key variable that affects the Borgsweer pressure match is the East permeability multiplier (*East_k_Mult*). To improve the Borgsweer history-match this multiplier needs to be reduced, but this worsens the match to pressure and PNL data in the main field. As a potential solution, a separate permeability multiplier was introduced for the Borgsweer area. A reduction of the local permeability around Borgsweer brings the pressure in the desired direction but also reduces the injectivity in Borgsweer wells. Historical volumes can then not be injected.

Introducing a new fault seal multiplier instead of an extra permeability multiplier turned out to be a better solution. The large fault between Borgsweer and DZL-1 (Fault "INT_16" highlighted in Figure 24) was fully open in the model, i.e., did not have a transmissibility multiplier. The extra fault seal multiplier allows an improved match of the Borgsweer pressure without compromising the history-match to other data.

Figure 25 shows the simulated and measured pressure data for all Borgsweer wells. Only four of the pressure data points contribute to the SPG RMSE and therefore steer the history-match. The other SPG measurements did not have long enough close-in periods. The most recent BRW-5 SPG data point (18-02-2022: 107 bar) is matched well by the V7 model: 106 bar. The model pressure for BRW-5 is lower than measured for the points with short close in time labelled "measured after injection" in Figure 25. For other wells, like BRW-2 and BRW-2A, the model pressure is higher than measured, for valid SPGs as well as pressure measurements with short close-in time. The final V7 model is considered a good compromise. The SPG RMSE for Borgsweer has reduced from 12.8 bar for V6 to 6.6 bar for V7.

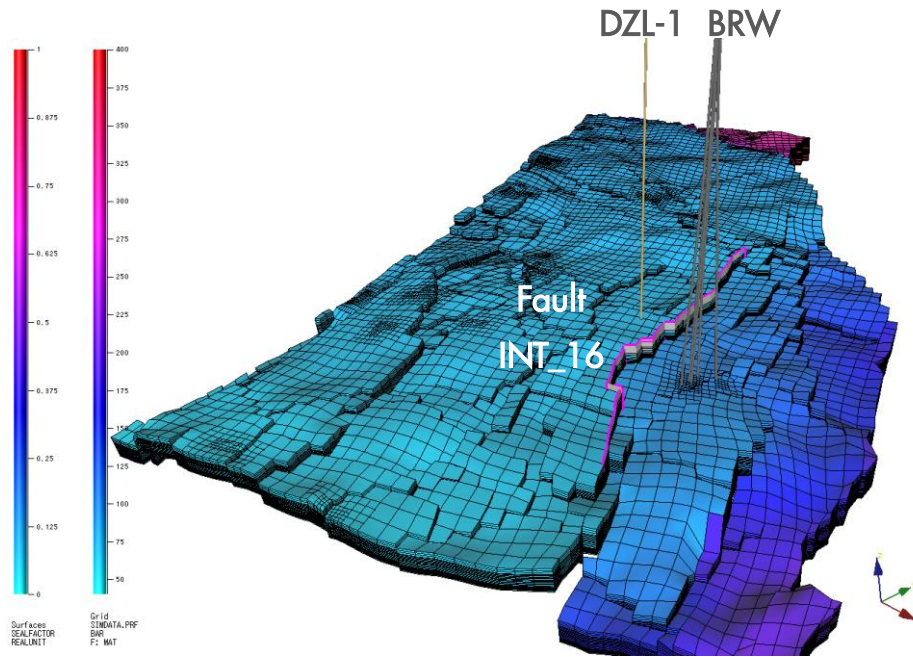


Figure 24: Fault INT_16 between DZL-1 and Borgsweer, on which a new fault seal factor (LogFaultSeal_BRW) is applied.

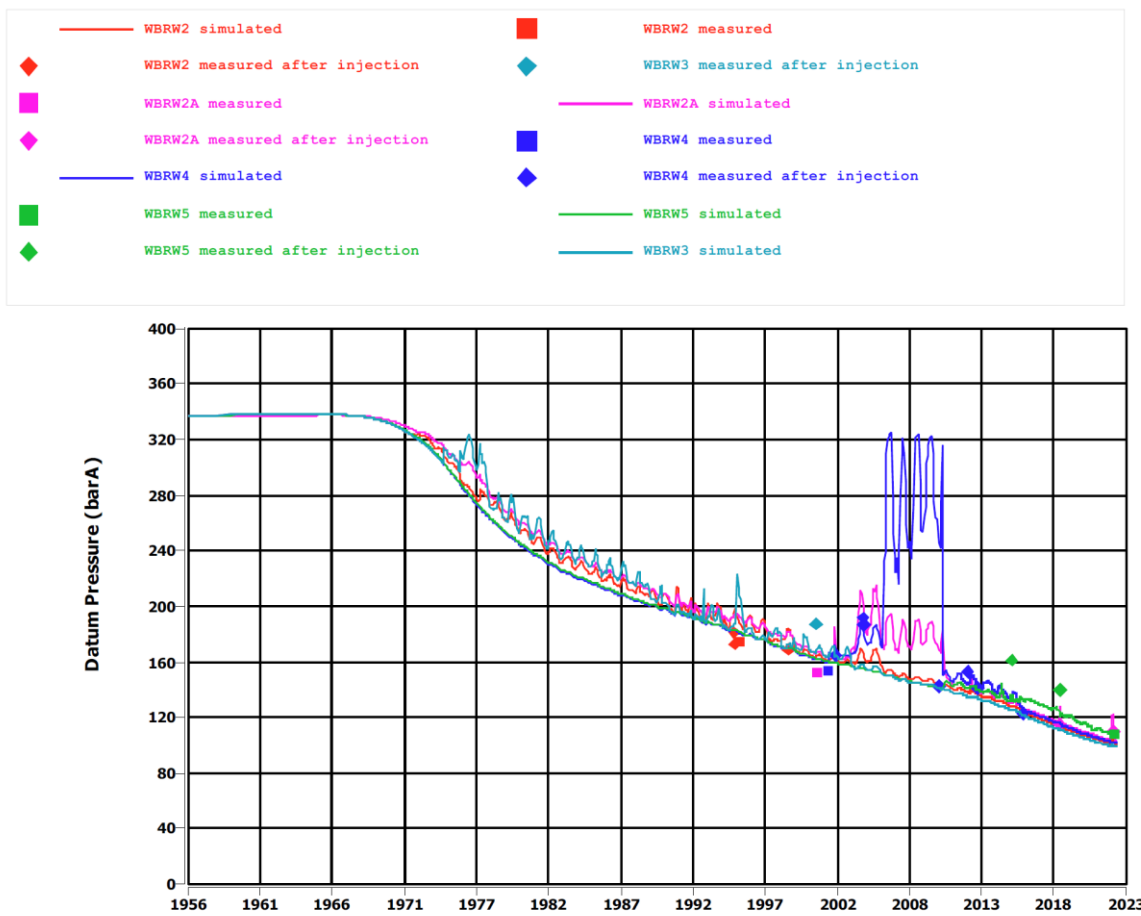


Figure 25: Comparison of simulated and measured pressures for Borgsweer wells. The pressure measurements labelled "measured after injection" have too short close-in times to be considered valid SPG data points.

The reduced transmissibility between DZL-1 and Borgsweer also slows down the encroachment of water and GWC rise in DZL-1. The GWC rise interpreted from PNL data in DZL-1 was poorly matched in the V6 model. With the fault adjustment a very good match to this data is now obtained, as shown Figure 26.

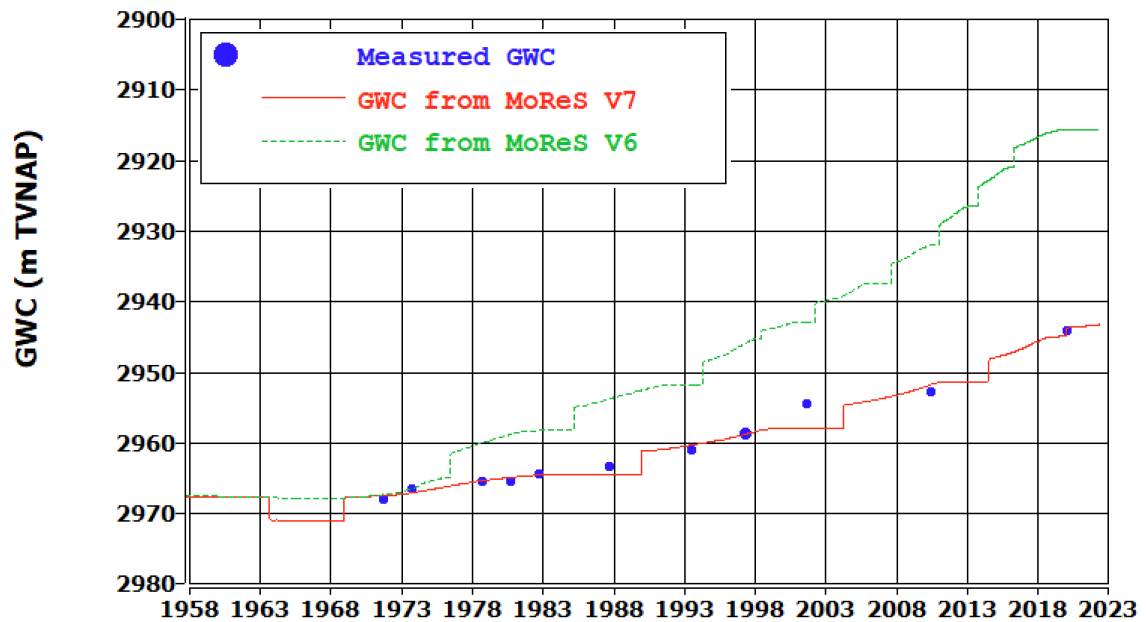


Figure 26: Improved match to PNL data DZL-1.⁷

⁷ The GWC calculated in MoRes sometimes shows stepwise rather than gradual changes. This is because the model struggles to resolve the exact position of the GWC due to the limited vertical grid resolution.

6 History-Match Results

Appendix A contains the complete set of history match plots for model V7. Appendix B lists the values of the input variables used. This chapter highlights some of the key results.

6.1 Overview

6.1.1 GIIP

The Groningen V7 model GIIP distribution is compared to that of V6 in Table 6. The Rotliegend GIIP in the V6 and V7 models are very close. The implementation of a paleo contact restricting the presence of gas-in-aquifer to a certain depth did not result in a larger optimal value of the gas saturation below the FWL. As a result, the V7 model has significantly less GIIP below the FWL than model V6. The larger GIIP in the Carboniferous is still well within the expected range of 20 to 70 NBcm [1].

Table 6: Groningen model GIIP distribution (NBcm).

| | V6 | V7 |
|----------------------------|--------|--------|
| Rotliegend above FWL | 2859.5 | 2853.0 |
| Rotliegend below FWL (PRG) | 175.3 | 62.2 |
| Carboniferous | 42.4 | 55.5 |
| Total | 3077.2 | 2970.7 |

6.1.2 Global history-match

Table 7 compares the global history-match of model V7 to that of V6. The RMSE for each data set is calculated as described in Section 4.3. The V6 RMSE values in Table 7 are larger than reported previously [1] due to corrections in some of the calculations. The largest difference is in the RMSE for the PNL data, as described in Section 4.3.4.

Table 7: Field-wide history match quality for the V6 and V7 models.

| Data set | Unit | RMSE V6 | RMSE V7 |
|-------------------------|----------------------------|---------|-------------------|
| SPG | bar | 2.8 | 2.3 |
| PNL (interpreted GWC) | m | 10.4 | 8.6 |
| RFT | bar | 9.8 | 7.4 |
| CiTHP | bar | 1.9 | 1.8 |
| Subsidence ⁸ | cm | 2.1 | 2.4 |
| Strain ZRP-3 | ($\mu\text{m}/\text{m}$) | 24.2 | 18.8 ⁹ |
| Gravity (All) | (μGal) | 5.0 | 5.1 |
| Gravity (Carboniferous) | (μGal) | 7.9 | 7.6 |

The overall match to the pressure data (SPG, RFT, and CiTHP) has improved compared to V6. The match to gravity data is similar and not further discussed in this report. The subsidence match (discussed in more detail in Section 6.7) was somewhat better in model V6, but the difference in the global RMSE for subsidence data is only a few mm. The match to the ZRP-3 strain data has significantly

⁸ Using C_m -porosity relation for both V6 and V7 models. V7 uses the 2018 survey, whereas V6 uses the 2013 survey, both in comparison to the 1972 survey.

⁹ Based on larger data set.

improved, even with a substantially larger data set used in the V7 comparison. A good match to the ZRP-3 strain data could only be obtained in the Rotliegend and not in the Carboniferous, as explained in Section 6.5.

6.1.3 Regional SPG pressure match

The RMSE for the SPG data is calculated for each of the Groningen pressure monitoring regions. These regions are described in the Groningen surveillance requirements [6] and monitoring strategy [7] documents. To ensure the SPG data was matched over the entire field-life, including recent periods with more sparse data, each decade with data contributed equally to the calculated RMSE (see Section 4.3.1).

Table 8 lists the V6 and V7 model SPG RMSE per monitoring region, with the included clusters, fields, or observation wells. The V6 and V7 RMSE use the same data sets and calculations. Zuidwending is listed separately since this area is part of the Groningen field but not part of a monitoring region [6].

Table 8: SPG RMSE for the Groningen pressure monitoring regions, other gas fields in the model, and Borgsweer.

| Region | Clusters/Fields/Observation wells | RMSE V6 | RMSE V7 |
|----------------------|--|----------------|----------------|
| South-West Periphery | EKL cluster, EKL-13, HRS-2A, KHM-1, TBR | 3.4 | 3.0 |
| South-West | FRB, KPD, SAP, SLO, TUS, SPH-1, WBL-1 | 1.4 | 1.3 |
| North-West | OVS, PAU, POS, BRH-1, ODP-1, SDM-1, ZRP-1 | 1.8 | 1.5 |
| North-East | BIR, LRM, ZND, HND-1, UHM-1A, UHZ-1 | 1.7 | 1.2 |
| Central-East | AMR, OWG, SCB, SDB, TJM, BOL-1, DZL-1, SMR-1 | 1.3 | 1.4 |
| South-East | EKR, MWD, NWS, ZPD, HGL-1, OLD-1 | 2.5 | 2.3 |
| South-Central | NBR, SPI, SZW, UTB, ZVN, MDN-1, ROT-1A | 1.9 | 1.7 |
| Zuidwending | ZWD-1, ZWD-2A | 4.8 | 3.4 |
| Land gas fields | Annerveen, Usquert, Zuidwending East (OPK-4A), Bedum, Feerwerd, Kielwindeweer, Warffum | 7.5 | 5.2 |
| Borgsweer | | 12.8 | 6.6 |

The RMSE for Land gas fields is the average of the RMSE's of 7 gas fields that are in the vicinity of Groningen and part of the Groningen dynamic model. The Midlaren field is excluded (but part of the overall SPG RMSE reported in Table 7) and discussed separately in Appendix D.

Model V7 has a comparable or improved SPG match in each region. The improvements in Bedum and Borgsweer have already been discussed in Sections 5.2 and 5.4. The executive summary includes a map that displays the data from Table 8 for the Groningen monitoring regions.

6.2 New SPG data

The model calibration used data up to May-2022. Since then, a few new pressure points have become available. These have been included in the SPG plots in Appendix A, for which the model has been run with production data up to 1-5-2023. The model match to most of the new data points is excellent, as shown in Table 9.

Table 9: V7 model match to newly acquired pressure data.

| well | type | date | measured pressure (bar) | simulated pressure (bar) | Δ (simulated – measured) (bar) |
|-------|------|------------|-------------------------|--------------------------|---------------------------------------|
| LRM-7 | LTMG | 16-05-2022 | 78.4 | 77.4 | -1.0 |
| BDM-5 | SPG | 23-09-2022 | 113.2 | 113.8 | 0.6 |
| BRH-1 | SPG | 04-10-2022 | 79.0 | 78.0 | -1.0 |
| SMR-1 | SPG | 11-10-2022 | 68.7 | 71.7 | 3.0 |
| SWO-1 | SPG | 14-10-2022 | 71.8 | 71.1 | -0.7 |
| KHM-1 | SPG | 08-03-2023 | 146.6 | 145.8 | -0.8 |

6.3 LTMG data Loppersum clusters

Appendix A contains SPG history-match plots for each cluster and observation well over the full lifetime of the Groningen field. The recent pressure data from memory gauges in wells LRM-7, OVS-5, PAU-2, and ZND-3 is part of the SPG data set and included in these plots. Figure 27 shows the recent history with SPG and LTMG data for these four wells in more detail. The history-match for the LTMG data is good, like it was for the V6 model. The SPG RMSE for each of the clusters LRM, PAU, OVS, and ZND is around 1 bar.

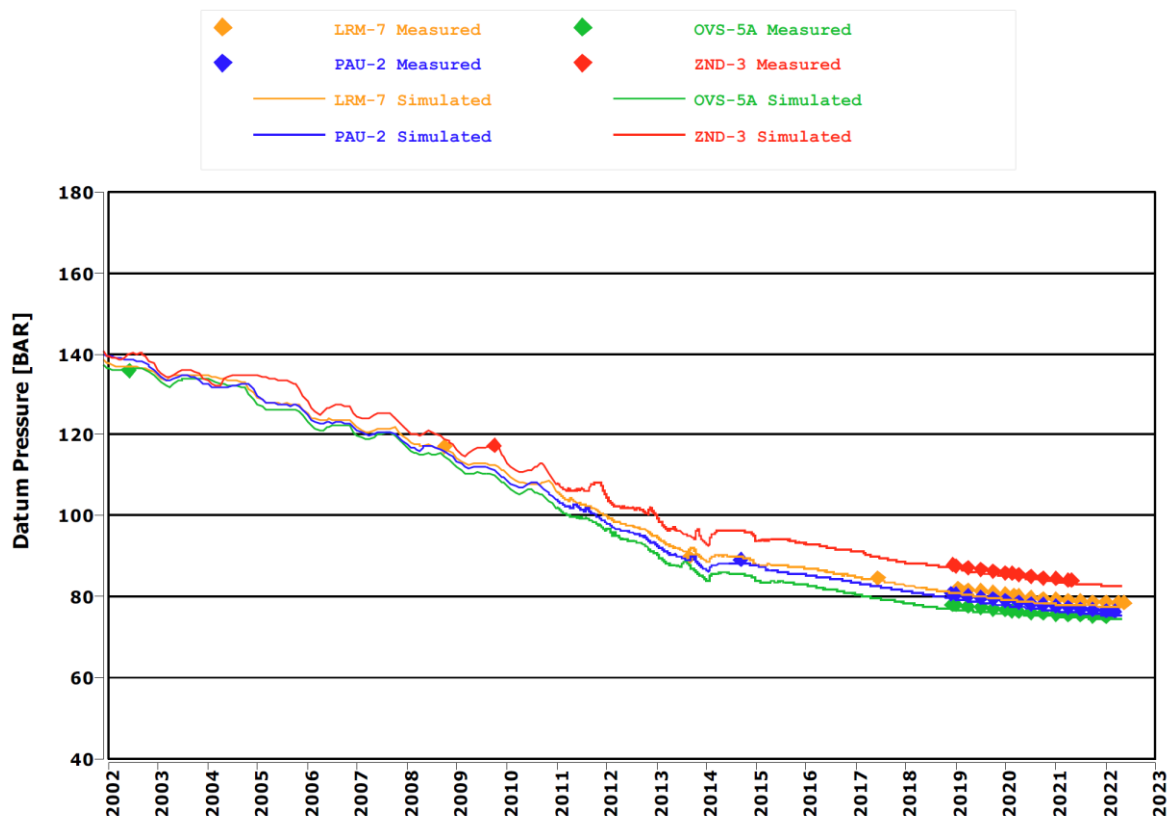


Figure 27: SPG and LTMG data in last 20 years for wells LRM-7, PAU-2, OVS-5A, and ZND-3.

6.4 Carboniferous depletion

One of the last history-matching cycles focused on fine-tuning of the Carboniferous properties. Figure 28 displays the Carboniferous horizontal and vertical permeability multipliers for all 660 runs in the space filling experimental design of Cycle 20. The top 25% of cases for the best field wide SPG match are highlighted in blue in the plot. (Note that all SPG data originates from the Rotliegend.) The cases with the best match to SPG data fall within a certain band, in which the vertical Carboniferous permeability needs to be smaller for larger Carboniferous horizontal permeability and vice versa. To obtain the best match to the SPG data a certain amount of Carboniferous depletion is required, but this can be achieved in various ways. Either with a lower Carboniferous horizontal permeability and higher vertical permeability, or with a higher Carboniferous horizontal permeability and lower vertical permeability.

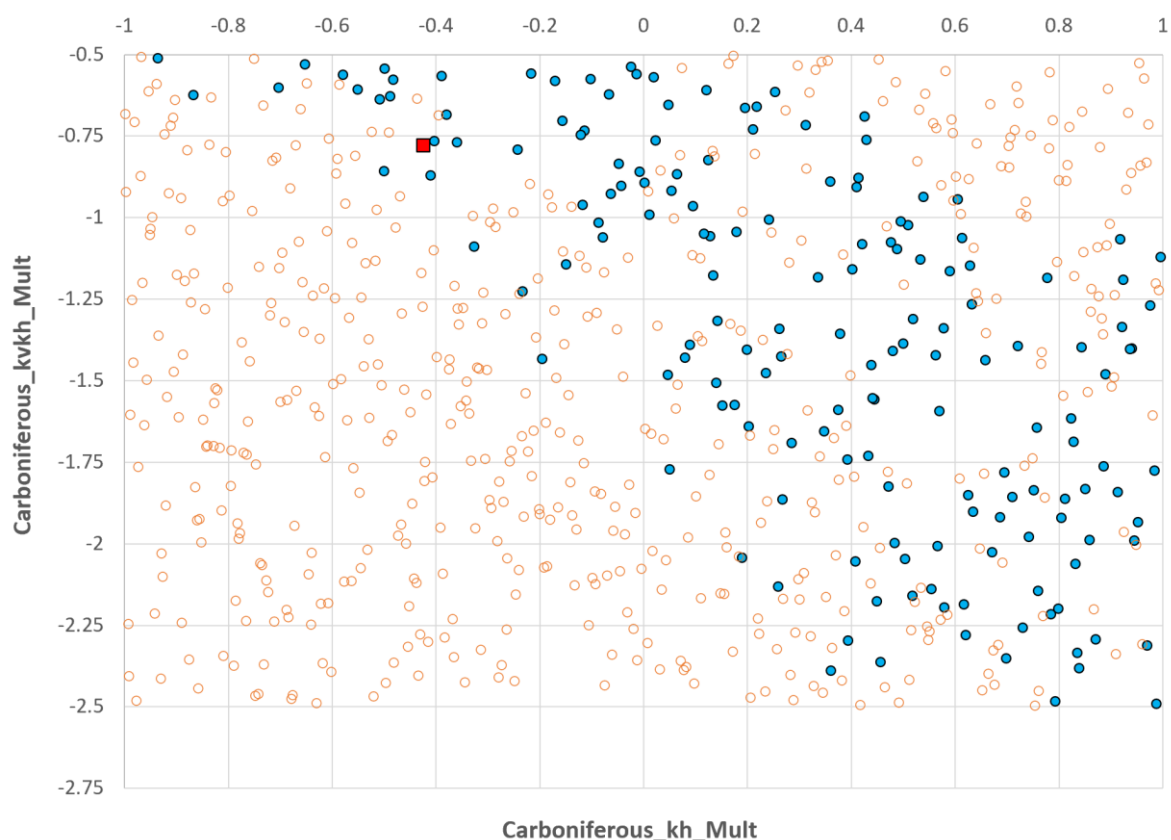


Figure 28: Experimental Design #20 with 660 runs. Highlighted in blue are the top 25% of best matches to SPG data (Field SPG RMSE < 2.47). The red square shows the final V7 model Carboniferous permeability multipliers.

The final V7 model permeability multipliers are shown in Figure 28 as well. This case was chosen because, among the models with a good fit to the SPG data, it gave the best overall match to the RFT data. The RFT data set used in the V7 history-match contains Carboniferous pressure data for 8 wells which were mostly of good but at least fair quality [13]: BOL-1¹⁰, HGZ-1, KPD-4A, KWR-1A, MDN-1, NWS-2, ZBR-1, and ZPD-1. The Carboniferous RFT data was excluded in the V6 history-match. Most wells with Carboniferous pressure data show no or very limited depletion, with a few exceptions.

The Carboniferous is modelled with uniform properties (NTG, porosity, permeability, compressibility). A transmissibility reduction is applied across the Rotliegend-Carboniferous boundary plane (through

¹⁰ The BOL-1 FIT data has been reported as taken in the Slochteren at 2893 m TVNAP [14]. However, this depth is well below the picked top of the Limburg (2845 m TVNAP).

variable *Carboniferous_horizon_Mult*). The interface between the Carboniferous and Rotliegend is an angular unconformity, which is not captured in the model [1]. There are locally some sands in the Carboniferous that are depleting through contact with the Rotliegend. Local variations in the Carboniferous are not captured in the uniform model. The main reason for the simplified modelling strategy of the Carboniferous is the lack of data. Further details can be found in the V6 model report [1], which introduced the Carboniferous in the Groningen model.

The Carboniferous properties can be tuned to decrease or increase the overall level of Carboniferous depletion to improve the history-match. As can be expected, the final model cannot match the carboniferous RFT data in all wells. For example, the model gives too much depletion compared to the data for ZBR-1 (Figure 29), and not enough depletion in BOL-1 (Figure 30). The KPD4A data, which shows a little depletion, is well matched (Figure 31). The final model was considered the best compromise. A full comparison between the model and RFT data for all wells is given in Appendix A.

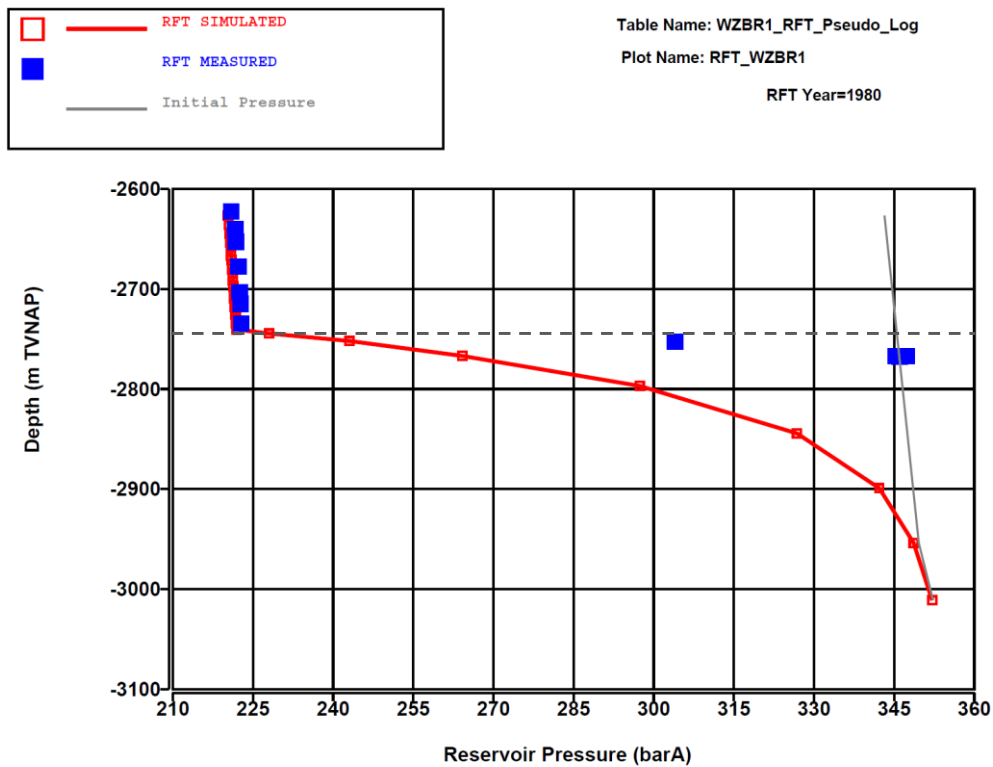


Figure 29: ZBR-1 RFT data compared to V7 model. The dashed line corresponds to the Rotliegend-Carboniferous interface.

Figure 32 shows the pressure in the upper part of the Carboniferous at the end of the history-match period for models V7 (left) and V6 (right). In model V6, depletion takes place mainly along large faults, where Carboniferous and Rotliegend are juxtaposed. This effect is still seen in model V7, but with an overall higher level of depletion. The match to the gravity data above the Carboniferous is slightly (5%) better for model V7.

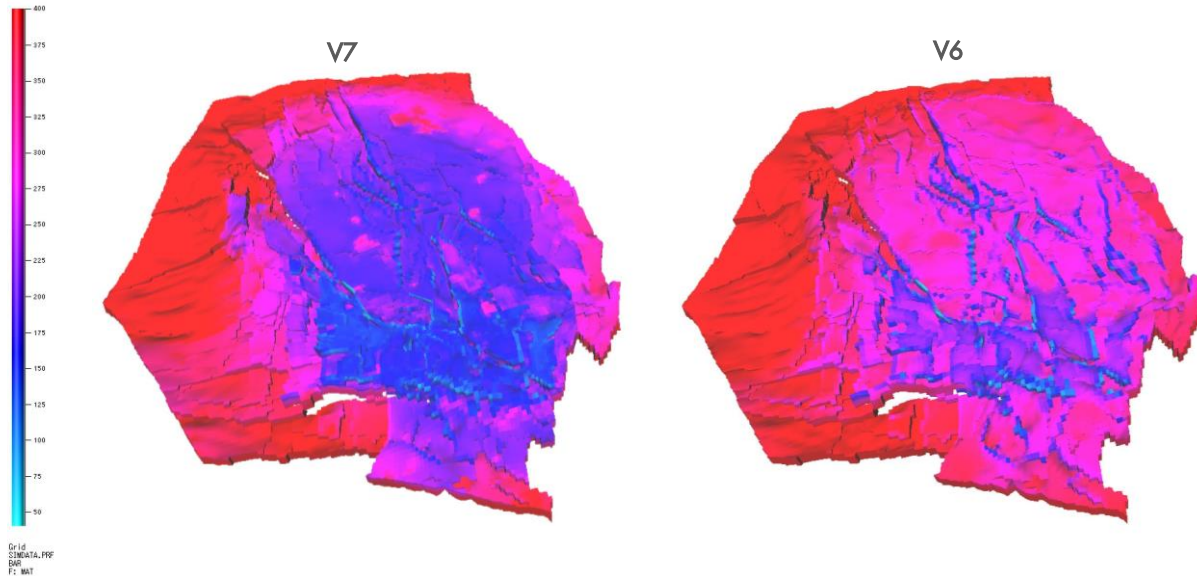


Figure 32: Comparison of Carboniferous pressure (on 1-5-2022) in V7 and V6 models. The top three Carboniferous model layers (30-35m) have been removed in this view.

6.5 DSS data

ZRP-3 strain data has been post-processed for comparison to the dynamic model, in a similar way as described for model V6 [11]. Five data sets are used to calculate the total DSS RMSE (Section 4.3.6). Three of these are shown in Figure 33: cumulative strain after 1, 3, and 5 years (with reference date 01-05-2016).

The measured cumulative strain is that averaged along the ZRP-3 trajectory across each model grid block. The model strain is calculated based on the grid block ΔP (compared to grid block pressure on 01-05-2016) and the rock compressibility C_m . The compressibility is porosity-dependent in the Rotliegend (see Section 4.2.9, [Eq. 3]) and a constant in the Carboniferous. The signature in the strain data for the Rotliegend is well matched. There is a little depth discrepancy between the average depth along the well trajectory used for measured strain, and the grid block centre used for model strain.

The model cannot reproduce the shape of the strain curves in the Carboniferous. The data shows a gradual decline of strain with depth into the Carboniferous (dashed lines in Figure 33). The simulation however always shows higher strain at the bottom than at the top of the Carboniferous (solid lines in Figure 33). With uniform porosity and compressibility, strain in the Carboniferous is linearly dependent on ΔP . In the lower part of the Carboniferous, where the pressure is still high, the model pressure declines by about 3 bar/year. In the upper part of the Carboniferous, the model pressure declines by about 2 bar/year. As a result, the calculated model strain increases with depth in the Carboniferous. This is true for all Carboniferous input variable combinations tested. The Carboniferous permeabilities affect the shape of the strain curve, and the compressibility its exact position, but the direction remains the same in all cases. This is a limitation of the simplified and uniform model description of the Carboniferous.

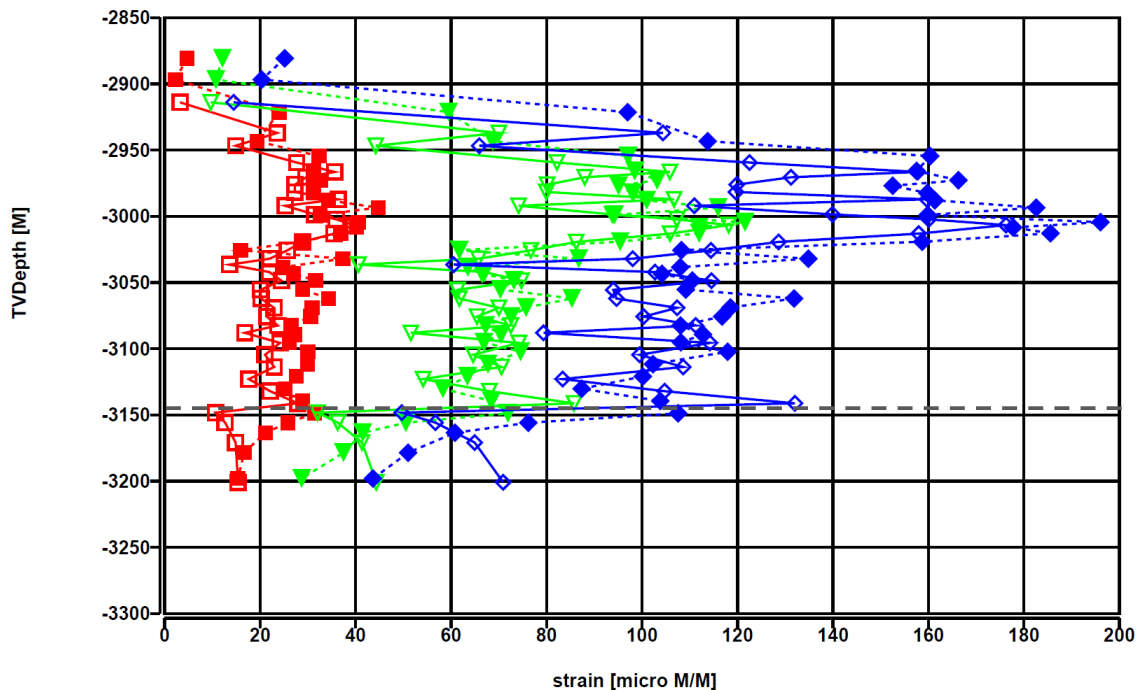
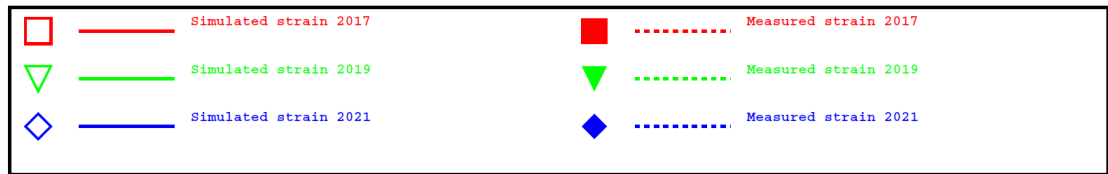


Figure 33: Model match to ZRP-3 in-situ strain. The dashed line corresponds to the Rotliegend-Carboniferous interface.

6.6 Southern Lauwerszee Aquifer

6.6.1 Fault seal factors

The Southern Lauwerszee aquifer in the south-west of the model has seven large (SW-NE trending) faults for which transmissibility is controlled by a single parameter: *LogFaultSeal_SWaquifer*. In the V6 model these faults were essentially closed (*LogFaultSeal_SWaquifer* = -4.0, i.e., a transmissibility multiplier of 0.0001). Figure 34 shows the location of these faults and well SAU-1. The RFT match of SAU-1 depends solely on the *LogFaultSeal_SWaquifer* parameter.

Figure 35 shows the effect of changing *LogFaultSeal_SWaquifer* from fully open (0) to closed (-4). A good match to the SAU-1 RFT data requires a partially sealing fault, with optimal *LogFaultSeal_SWaquifer* between -1 and -2. The final V7 model uses *LogFaultSeal_SWaquifer* = -1.3, corresponding to a fault transmissibility multiplier of 0.05.

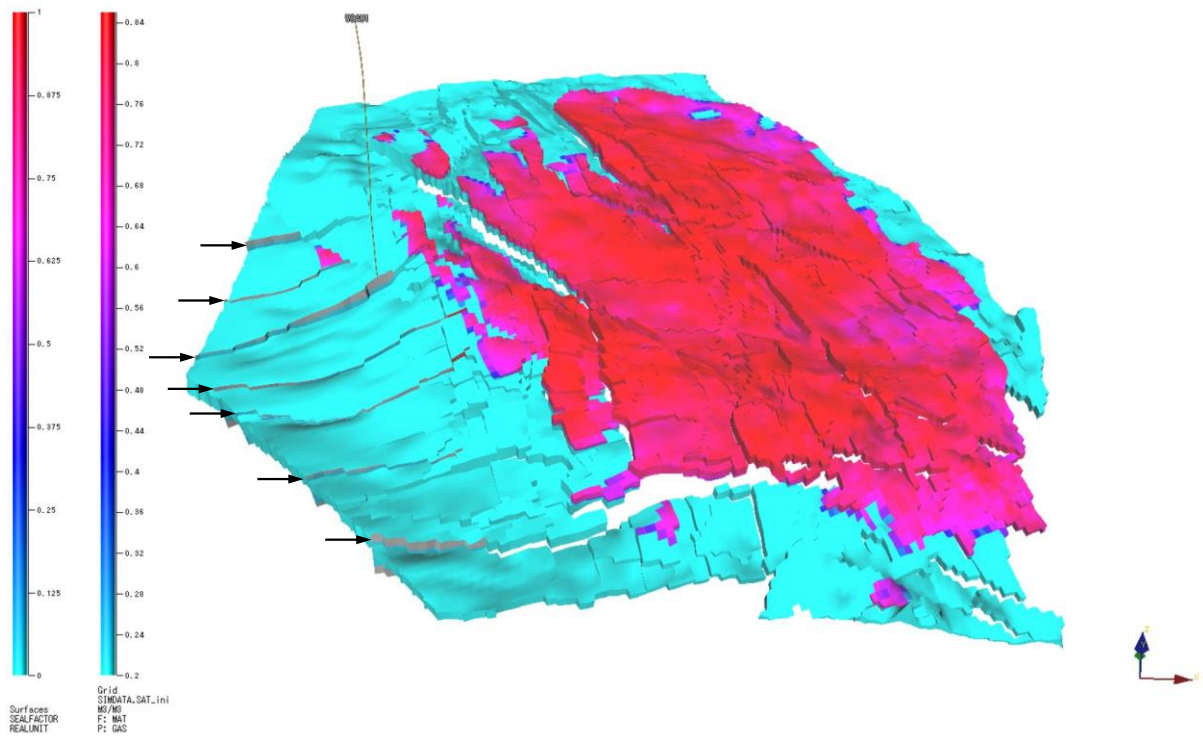


Figure 34: Seven faults in the Southern Lauwerszee aquifer, for which transmissibilities are controlled by *LogFaultSeal_SWaquifer*. Shown is initial saturation in the Slochteren (ROSL) and the well trajectory for SAU-1.

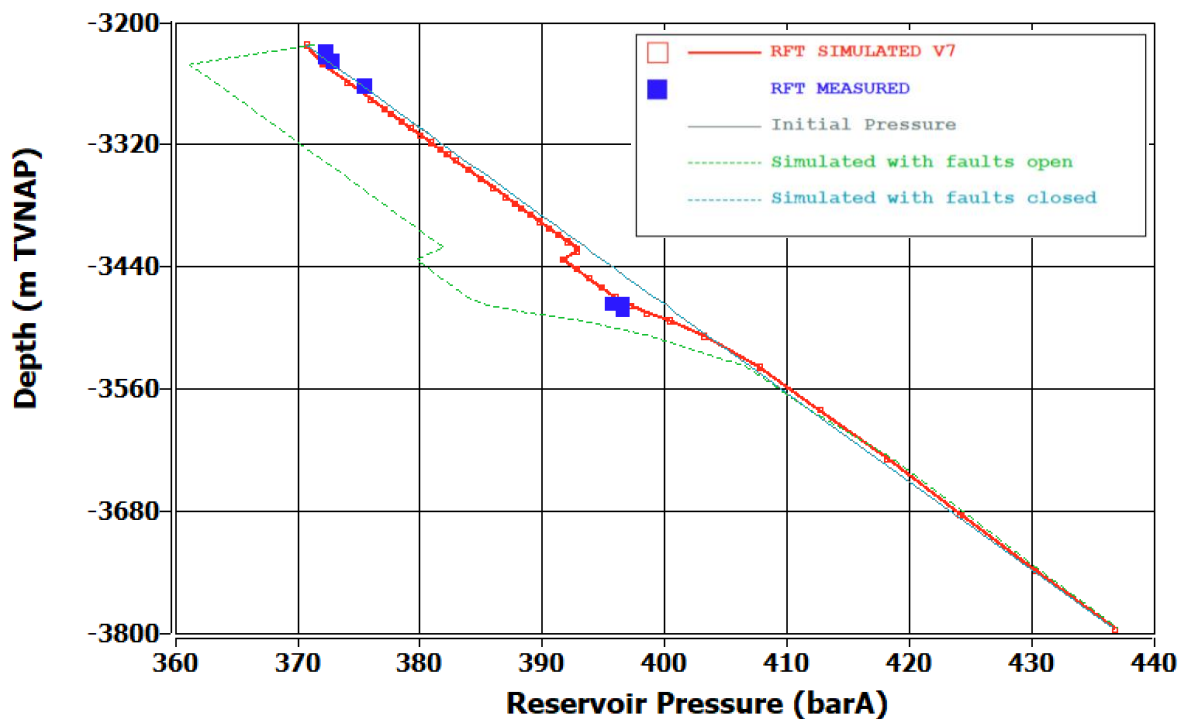


Figure 35: Comparison of SAU-1 RFT (28-11-1995) to simulated pressure profile for open faults (*LogFaultSeal_SWaquifer* = 0), closed faults (*LogFaultSeal_SWaquifer* = -4.0), and the V7 model with partially open faults (*LogFaultSeal_SWaquifer* = -1.3)

6.6.2 Pseudo-aquifer wells

Section 4.2.5 described the pseudo-aquifer wells introduced in model V6 to incorporate depletion in the Southern Lauwerszee aquifer due to gas fields to its west. The scaling factors that control the offtake of the pseudo-aquifer wells were continued to be used in the V7 history-match. For most of them, similar optimal values have been obtained as in V6. See for a comparison of V7 values to those of V6 the table in Appendix B.

Sensitivities were performed on the final V7 model, testing the effect of a 50% increase or decrease in offtake related to the fields Faan, Pasop, Roden, and Vries. These fields are located to the southwest of the Groningen field and shown in Figure 6. Selected results are summarized in Table 10. The values listed for the total SPG RMSE exclude the Midlaren location, to illustrate that only the Midlaren pressure match is affected when pseudo-aquifer well offtake associated with the Roden or Vries fields is changed. The MLA-1 observation well location to the southwest of the Groningen field is shown in Figure 1. The Midlaren field is a special case and further discussed in Appendix D.

Table 10: Pseudo-aquifer well sensitivities.

| Case | Total SPG RMSE Excluding MLA-1 (bar) | Subsidence RMSE (cm) | SPG RMSE MLA-1 (bar) |
|---------------------------|--|-------------------------|-------------------------|
| V7 base case model | 2.151 | 2.41 | 14.262 |
| Faan +50% | 2.151 | 2.41 | 14.262 |
| Faan -50% | 2.152 | 2.42 | 14.262 |
| Pasop +50% | 2.151 | 2.40 | 14.261 |
| Pasop -50% | 2.151 | 2.43 | 14.261 |
| Roden +50% | 2.151 | 2.41 | 11.911 |
| Roden -50% | 2.150 | 2.42 | 17.563 |
| Vries +50% | 2.151 | 2.42 | 13.385 |
| Vries -50% | 2.151 | 2.42 | 17.397 |

The global history-match for SPG, subsidence, and all other data sets is very insensitive to the pseudo-aquifer well parameters. This insensitivity means that similar quality history-matches can be achieved with different levels of pseudo-aquifer well offtake. There is a relatively large uncertainty around the level of aquifer depletion due to the lack of data. There are no pressure measurements in the aquifer, only indirect subsidence data.

6.7 Subsidence match

The subsidence proxy model allows the use of subsidence data in the dynamic model history-matching process. This simplified model does not describe subsidence as well as the geomechanical model that NAM uses for subsidence predictions [5]. The proxy model calculates subsidence (in 2018 with reference to 1972) based on the simulated pressure differentials, rock compressibility, and a few other parameters that are fixed in the model [2]. The rock compressibility values measured on core plugs need to be scaled down for the proxy model to match the subsidence data.

In the V6 model, the Rotliegend scaling factor (*Compress_rock_mult*) was 0.40. For the V7 model it is slightly lower (0.34), but V7 also uses a new subsidence dataset and updated Rotliegend rock compressibility equation. A similar scaling factor has now been introduced for the Carboniferous (*Compress_rock_Carb_mult* = 0.42).

The Rotliegend compressibility is a function of porosity ([Eq. 3] in Section 4.2.9) and the Carboniferous compressibility is uniform ($Compress_rock_Carb = 0.50 \cdot 10^{-5}$ bar). In model V6, minimum and maximum values for the (porosity-dependent) Rotliegend compressibility were introduced based on the experimental data ranges (see Figure 7-18 in the V6 report [1]). A QC plot was developed to identify areas in which subsidence could not be matched within the expected range of Rotliegend compressibility. (Subsidence is dominated by Rotliegend compaction, the Carboniferous effect is small in comparison.)

Figure 36 shows a similar QC plot for the V7 model compared to that of V6. For most of the model the subsidence data can be matched within the minimum to maximum compressibility range. The green areas for which a small mismatch remains are mostly at the boundary of the dynamic model grid or at the boundary of the area for which subsidence data exists.

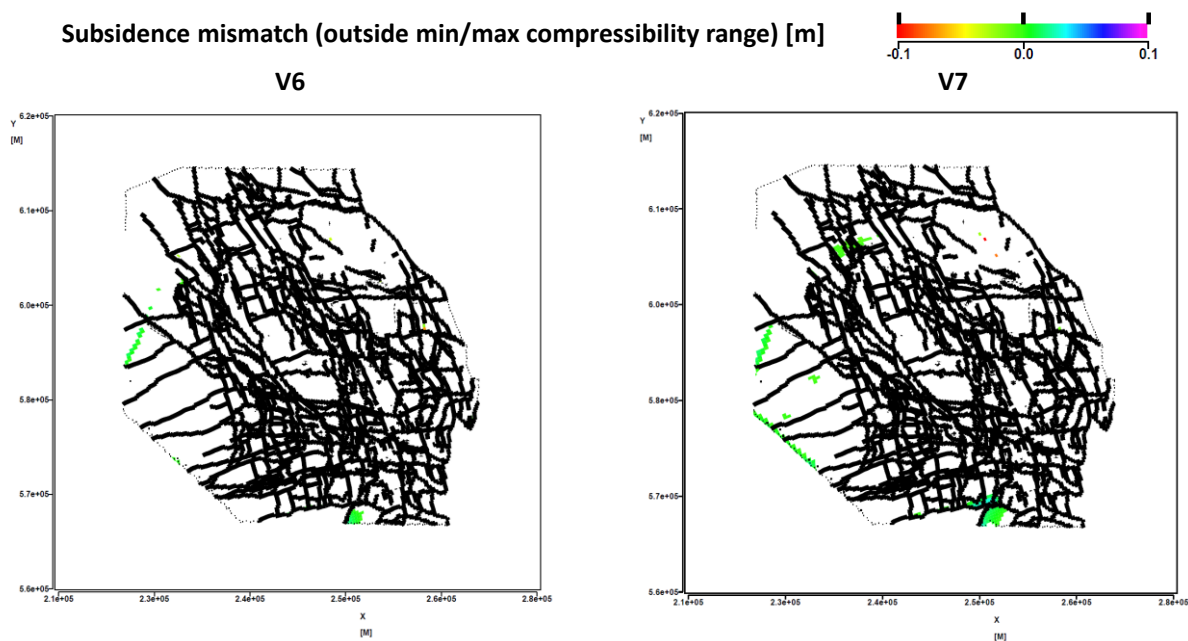


Figure 36: Subsidence mismatch remaining in V6 model (left) and V7 model (right) when using the minimum or maximum compressibility values. For V6 subsidence in 2013 is shown, for V7 subsidence in 2018, both with respect to the 1972 survey.

For models V5 and V6 the subsidence data match was improved through a close-the-loop exercise. Reservoir pressures from an (intermediate) best-match model were exported and used in the geomechanical model that is used for subsidence predictions. The final rock compressibilities from subsidence inversion were loaded back into the dynamic model. Using this updated C_m grid, instead of the porosity-dependent relationship, improved the proxy model subsidence match (as illustrated for example in Fig. 4-19 of the V5 model report [3]). Due to resource and time constraints, such a close-the-loop exercise has not been done for model V7. The geomechanics team did perform a quick analysis using the V7 model pressure output that confirmed a similar match to subsidence data can be achieved as with the use of V6 model output.

More work is required to incorporate the V7 dynamic model output into the geomechanics model for the North of the Netherlands and recalibrate this model. This work will be done for the next update of the subsidence forecast for the North of the Netherlands in 2025.

7 Conclusions

The Groningen V7 dynamic model is based on static model Petrel_V7 which includes several corrections compared to Petrel_V6. The V7 MoReS model has been calibrated using available data up to 1-5-2022. It has a comparable or improved history-match compared to model V6 for each data set. For each pressure monitoring region in the Groningen field (including the Southwest periphery), the RMSE for SPG data is now within 3.0 bar.

The most significant improvement is the KHM-1 pressure history-match. In contrast to the V6 model, the V7 model matches both early and late data, including the latest SPG data (March-2023) that was not used in the history-match. The history-match for both Borgsweer pressure and DZL-1 GWC rise has been improved in one-go through introduction of a single fault seal factor.

The V7 dynamic model will be used to generate pressure distribution forecasts, which serve as input for i) subsidence forecasting (by NAM's geomechanical team), and ii) TNO's seismic hazard and risk assessments.








The largest uncertainty in the modelled pressure distribution is in the aquifers surrounding the field, and the Carboniferous formation. There is very limited data in these areas to constrain the model.

Pressure monitoring in the Groningen field will continue as described in the monitoring strategy [7]. These pressure measurements will be compared in future to the V7 model pressure. NAM reports this data and comparison to SodM every two years.

8 References

- [1] Q. de Zeeuw and L. Geurtsen, "Groningen Dynamic Model Update 2018 - V6," NAM, EP201809202872, Assen, 2018.
- [2] U. Burkitov, H. van Oeveren and P. Valvatne, "Groningen Field Review 2015 Subsurface Dynamic Modelling Report," NAM, EP201603238100, Assen, 2016.
- [3] Q. de Zeeuw and L. Geurtsen, "Groningen Dynamic Model Update 2017 - V5," NAM, EP201806200206, Assen, 2018.
- [4] E. Fokkema, "Groningen Carboniferous development petrophysics 2004-2006," NAM, EP200702208099, Assen, 2007.
- [5] Nederlandse Aardolie Maatschappij B.V., "Groningen long term subsidence forecast," NAM, EP202008201822, Assen, 2020.
- [6] L. Geurtsen, A. J. Landman and G. Ketelaar, "Groningen abandonment - Surveillance requirements," NAM, EP202006201318, Assen, 2020.
- [7] Nederlandse Aardolie Maatschappij B.V., "Monitoring Strategie Groningenveld," NAM, 2020.
- [8] H. van Oeveren, P. Valvatne and L. Geurtsen, "Groningen Dynamic Model Update 2017," NAM, EP201708205454, Assen, 2017.
- [9] Q. De Zeeuw, "CITHP to CIBHP conversion for the Groningen wells," NAM, EP201512250703, Assen, 2016.
- [10] J. Geertsma and G. van Opstal, "A Numerical Technique for Predicting Subsidence above Compacting Reservoirs, based on the Nucleus of Strain Concept," Koninklijke Shell Exploratie en Productie Laboratorium, Publication 405, Rijswijk, 1972.
- [11] P. Kole, "Strain data obtained by Zeerijp-3A DSS for implementing in Groningen RE model," NAM, EP201806209144, Assen, 2018.
- [12] H. Van Oeveren, "Implementation of time-lapse gravity data in the Groningen dynamic model," NAM, EP201704204007, Assen, 2017.
- [13] L. Vos, "Groningen Field RFT and FIT Data & Information on Limburg Connectivity," NAM, EP200603207569, Assen, 2003.
- [14] Nederlandse Aardolie Maatschappij B.V., "A review of FIT's and RFT's performed in the GRONINGEN field," NAM report no. 89.2.458, Assen, 1989.

Appendix A V7 best match

| | |
|--|---|
| <p>SPG match</p> <p>RMSE = 2.26 bar</p> |  GRO_V7_HM_vMay23_SPTG.pdf |
| <p>RFT match</p> <p>RMSE = 7.43 bar</p> |  GRO_V7_HM_vMay23_RFT.pdf |
| <p>CITHP2BHP match</p> <p>RMSE = 1.84 bar</p> |  GRO_V7_HM_vMay23_CITHP.pdf |
| <p>PNL match</p> <p>RMSE = 8.6 meter</p> |  GRO_V7_HM_vMay23_PNL.pdf |
| <p>Subsidence match</p> <p>RMSE = 2.4 cm</p> |  GRO_V7_HM_vMay23_Subs.pdf |
| <p>Gravity Match</p> <p>RMSE = 5.06 μGal</p> |  GRO_V7_HM_vMay23_Grav.pdf |
| <p>ZRP strain DSS</p> <p>RMSE = 18.75 μstrain</p> |  GRO_V7_HM_vMay23_DSS_Match.pdf |

Appendix B History-Match input variable values

| Input variable | V6 model value | V7 model value | Comment |
|--|----------------|----------------|--|
| <i>Grid block volume multipliers</i> | | | |
| NorthEast_gbv_Mult | 0.9949 | 1.0112 | |
| NorthWest_gbv_Mult | 0.9940 | 1.0151 | |
| East_gbv_Mult | 0.9948 | 0.9973 | |
| Central_gbv_Mult | 0.9822 | 0.9786 | |
| SouthWest_gbv_Mult | 1.005 | 1.004 | |
| SouthEast_gbv_Mult | 0.9800 | 0.9811 | |
| Eemskanaal_gbv_Mult | 1.0220 | 1.0059 | |
| Kolham_gbv_mult | 1.019 | 1.020 | |
| Harkstede_gbv_mult | 2.8450 | 3.3521 | |
| USQ_gbv_mult | 0.997 | 2.200 | |
| OPK4_gbv_mult | 1.82 | 1.72 | |
| BDM_gbv_mult | 0.866 | 0.86175 | |
| BDM_South_gbv_mult | | 0.60 | New variable in V7. See Section 5.2. |
| KWR_gbv_mult | 0.87 | 0.79 | |
| FWD_gbv_mult | 0.40 | 0.2035 | |
| WRF_gbv_mult | 1.00 | 1.04 | |
| ANV_gbv_mult | 0.7834 | 0.46 | |
| MLA_gbv_mult | 1.00 | 0.25 | |
| <i>(Log-)Permeability multipliers (see Section 4.2.2 for porosity-dependent implementation)</i> | | | |
| NorthEast_k_Mult | 0.9977 | 1.093 | |
| NorthWest_k_Mult | 0.99 | 1.25 | |
| East_k_Mult | 0.9578 | 1.115 | |
| Central_k_Mult | 1.0 | 1.0 | |
| SouthWest_k_Mult | 0.9488 | 1.0 | |
| SouthEast_k_Mult | 0.9750 | 0.985 | |
| Zeerijp_k_Mult | 0.99 | 1.32 | |
| Eemskanaal_k_Mult | 0.4766 | 0.516 | |
| Ameland_k_Mult | -1.0 | -2.8 | |
| NE_USS_Shale_k_mult | -1.0 | -1.0 | |
| Feerwerd_k_Mult | -1.0 | -1.29 | |
| Warffum_k_Mult | 0.96 | 1.24 | |
| Delta_k_North_ROSLL | | 0.125 | New (absolute) permeability multiplier. See Section 5.3. |
| <i>Carboniferous property modifiers</i> | | | |
| Carboniferous_horizon_Mult | -0.48 | -0.214 | |
| Carboniferous_por_mult | 1.325 | 1.475 | |
| Carboniferous_kvkh_Mult | -1.81 | -0.78 | |
| Carboniferous_kh_Mult | 0.0 | -0.424 | |
| Compress_rock_Carb | 0.30 | 0.50 | |
| Compress_rock_Carb_mult | | 0.416 | New variable in V7. See Section 4.2.3. |
| <i>Fault seal factors</i> | | | |
| LogFaultSeal_PosPau | -0.20 | -0.20 | |

| | | | |
|----------------------------|-------|-------|--|
| LogFaultSeal_USQ | -1.88 | -1.60 | |
| LogFaultSeal_USQ_N | -1.10 | 0.0 | |
| LogFaultSeal_ODP_NS | -2.00 | -2.40 | |
| LogFaultSeal_ODP_NWSE | -0.86 | -1.20 | |
| LogFaultSeal_ODP_WE | -1.66 | -1.90 | |
| LogFaultSeal_WRFi | -1.00 | -0.93 | |
| LogFaultSeal_WRF_N | -3.00 | -1.40 | |
| LogFaultSeal_UHZ_ZND | -1.27 | -1.24 | |
| LogFaultSeal_ZND_LRM | -1.32 | -1.42 | |
| LogFaultSeal_ZNDLRM_BIR | -0.90 | -0.90 | |
| LogFaultSeal_BRW | | -1.40 | New variable in V7. See Section 5.4. |
| LogFaultSeal_ZWD | -1.85 | -2.45 | |
| LogFaultSeal_ZWD12 | -1.00 | -0.90 | |
| LogFaultSeal_ERKcluster | -2.00 | -1.01 | |
| LogFaultSeal_ANV_N | 0.00 | 0.00 | |
| LogFaultSeal_OPK4 | -2.18 | -2.20 | |
| LogFaultSeal_KWR | -3.00 | -0.20 | |
| LogFaultSeal_PopUps | -0.10 | -0.10 | |
| LogFaultSeal_KpdWbl | -1.60 | -1.50 | |
| LogFaultSeal_FrbSap_E | -1.17 | -1.16 | |
| LogFaultSeal_SzwRot | -1.40 | -1.69 | |
| LogFaultSeal_HGZ | -1.14 | -0.38 | |
| LogFaultSeal_SPHWest | -0.50 | -0.64 | |
| LogFaultSeal_KHMTrough_WE | -2.31 | -2.23 | |
| Delta_KHMTrough_WE | | -0.36 | New variable in V7. See Section 5.1.3. |
| LogFaultSeal_HarkstedeGron | -0.03 | -0.40 | |
| LogFaultSeal_HRS_E | -0.71 | -0.60 | |
| LogFaultSeal_HRS_HRSNW | -0.65 | -2.0 | |
| LogFaultSeal_HRS_AQF | 0.00 | 0.00 | |
| LogFaultSeal_EKLW | -1.22 | -0.89 | |
| LogFaultSeal_HRS_TBR | -3.91 | -3.37 | |
| LogFaultSeal_EKL_N | -0.95 | -1.25 | |
| LogFaultSeal_TBR_N | -0.51 | -0.40 | |
| LogFaultSeal_RDW_NS | -2.55 | -3.00 | |
| LogFaultSeal_RDW_WE | -2.95 | -3.25 | |
| LogFaultSeal_BDM12_Gron | -1.30 | -2.60 | |
| LogFaultSeal_BDM12_4 | -1.48 | -1.10 | |
| LogFaultSeal_BDM5_Gron | 0.00 | -1.40 | |
| LogFaultSeal_BDM4_5 | -1.48 | -0.50 | |
| LogFaultSeal_BDM5_Swaqf | 0.00 | -2.00 | |
| LogFaultSeal_BDM12_3 | -2.18 | -2.50 | |
| LogFaultSeal_RANBDM3 | -1.79 | -2.00 | |
| LogFaultSeal_BDM3_N | -2.57 | -2.80 | |
| LogFaultSeal_RANW | -1.95 | 0.00 | |
| LogFaultSeal_BDMaqf | -3.00 | -4.00 | |
| LogFaultSeal_SWaquifer | -4.00 | -1.3 | |
| LogFaultSeal_MLA | 0.00 | 0.00 | |

| Aquifer parameters | | | |
|---|--------|--------|--|
| AqfLength_Moewensteert | 22500 | 22500 | Used for significance testing only. |
| AqfLength_Rodewolt | 15000 | 15000 | Used for significance testing only. |
| AqfLength_Rysum | 15000 | 15000 | Used for significance testing only. |
| AqfLength_Usquert | 7500 | 7500 | Used for significance testing only. |
| AqfVsc | 1.00 | 1.00 | Used for significance testing only. |
| Aqf_well_ROD_scale | 0.35 | 0.35 | |
| Aqf_well_VRS_scale | 0.25 | 0.32 | |
| Aqf_well_VRS47to8_scale | 0.50 | 0.50 | |
| Aqf_well_FAN_scale | 1.00 | 1.00 | |
| Aqf_well_PSP_scale | 1.00 | 0.60 | |
| Fluid densities | | | |
| density_gas | 197.0 | 197.0 | Used for significance testing only. |
| density_water | 1172.0 | 1172.0 | Used for significance testing only. |
| Relative permeability parameters | | | |
| Krw_at_Srg | 0.377 | 0.377 | Used for significance testing only. |
| Krg_at_Swc | 0.860 | 0.860 | Used for significance testing only. |
| Nw | 4.0 | 4.0 | Used for significance testing only. |
| Ng | 1.5 | 1.5 | Used for significance testing only. |
| Gas-in-aquifer parameters | | | |
| Paleo_contact | | 3185 | New variable in V7. See Section 5.1.2. |
| SGR_aqf | 0.030 | 0.023 | |
| Regional Free-Water-Levels | | | |
| FWL_Groningen_Central | 2992 | 3011 | |
| FWL_Groningen_E | 2972 | 2972 | Used in several cycles but finally kept as in V6. |
| FWL_Groningen_NE | 2978 | 2979 | |
| FWL_Groningen_NW | 2984 | 2984 | Used in several cycles but finally kept as in V6. |
| FWL_Groningen_SE | 3006 | 3006 | Used in several cycles but finally kept as in V6. |
| FWL_Groningen_SW | 2995 | 2995 | Used in several cycles but finally kept as in V6. |
| FWL_Gron_Eemskanaal | 2996 | 2996 | Used in several cycles but finally kept as in V6. |
| FWL_Gron_Ellerhuizen | 2997 | 2997 | Set to fixed value, i.e., not used in calibration. |
| FWL_Gron_Harkstede | 3016 | 3016 | Used in several cycles but finally kept as in V6. |
| FWL_Gron_Hoogezand | 3030 | 3030 | Used in several cycles but finally kept as in V6. |
| FWL_Gron_Oldorp | 2967 | 2967 | Used in several cycles but finally kept as in V6. |
| FWL_Gron_Zuidwending | 3017 | 3017 | Used in several cycles but finally kept as in V6. |
| Rotliegend compressibility multiplier for subsidence match (see Section 4.2.9) | | | |
| Compress_rock_mult | 0.40 | 0.339 | |

Appendix C Conversion of CiTHP to BHP

De Zeeuw developed correlations to calculate BHP from CiTHP for the Groningen wells in 2016 [9]:

$$CiBHP = M \cdot CiTHP$$

$$M = a_1 \cdot \log_{10}(t)^3 + a_2 \cdot \log_{10}(t)^2 + a_3 \cdot \log_{10}(t) + a_4$$

with t the close-in time in days.

The coefficients a_1 to a_4 used in these correlations have been updated for several clusters based on new data. The table below contains the values that are now used in the CiTHP to BHP calculation. These values replace those in Table 6 of the original document [9]. The clusters with an asterisk (*) have been updated.

| Cluster/Region | a_1 | a_2 | a_3 | a_4 |
|-------------------|----------|---------|--------|--------|
| Field | 0.000375 | -0.0038 | 0.0128 | 1.22 |
| AMR | 0 | -0.0016 | 0.0089 | 1.2161 |
| BIR* | 0 | -0.0032 | 0.0107 | 1.2109 |
| EKL* | 0 | -0.0052 | 0.0163 | 1.2183 |
| EKR* | 0 | -0.0019 | 0.0093 | 1.2222 |
| FRB | 0 | -0.0015 | 0.0068 | 1.2237 |
| KPD* | 0 | -0.0023 | 0.0085 | 1.2251 |
| LRM* | 0 | -0.0008 | 0.0071 | 1.2103 |
| MWD | 0 | -0.0019 | 0.0126 | 1.2158 |
| NBR* | 0 | -0.0051 | 0.0088 | 1.2297 |
| NWS* | 0 | -0.0034 | 0.0176 | 1.2132 |
| OVS | 0 | -0.0015 | 0.0093 | 1.2128 |
| OWG | 0 | -0.0015 | 0.0076 | 1.2190 |
| PAU* | 0 | -0.0045 | 0.0161 | 1.2128 |
| POS* | 0 | -0.0011 | 0.0085 | 1.2139 |
| ROT ¹¹ | 0 | 0.0000 | 0.0089 | 1.2100 |
| SAP | 0 | -0.0055 | 0.0241 | 1.2108 |
| SCB* | 0 | -0.0023 | 0.0124 | 1.2146 |
| SDB | 0 | -0.0048 | 0.0172 | 1.2153 |
| SLO | 0 | -0.0024 | 0.0098 | 1.2224 |
| SPI* | 0 | -0.0021 | 0.0091 | 1.2252 |
| SZW | 0 | -0.0028 | 0.0095 | 1.2238 |
| TJM* | 0 | -0.0006 | 0.0078 | 1.2157 |
| TUS | 0 | -0.0020 | 0.0112 | 1.2188 |
| UTB | 0 | -0.0018 | 0.0084 | 1.2263 |
| ZND | 0 | -0.0016 | 0.0109 | 1.2085 |
| ZPD | 0 | -0.0033 | 0.0132 | 1.2185 |
| ZVN | 0 | -0.0020 | 0.0101 | 1.2211 |

¹¹ Bad fit based on two conflicting data points [9]. No CiTHP2BHP data for ROT-1 used.

Appendix D Midlaren history-match

The Midlaren field with observation well MLA-1 depletes only through the aquifer. The limited pressure data available for MLA-1 is shown in Figure 37. The first data point plotted corresponds to the initial RFT in 1985. The subsequent three SPG data points all received the lowest possible quality score (1 out of 10). The second set of three SPG data points shows a constant pressure from 2002 to 2012. It was impossible to match this behaviour in both V6 and V7 models.

In MLA-1 only the Ten Boer is gas bearing (down to bottom ROCLT at 3173 m TVDSS). The Slochteren (ROSL) was found to be oil-bearing (37° API), down to 3197 m TVDSS. The two-phase Groningen MoReS model considers only gas and water and cannot capture this.

The Midlaren datum level is at 3190 m TVDSS. The SPG surveys measure water gradients (1.15 bar/10 m). Model V6 used a datum level of 3175 m TVDSS (approximate bottom of ROCLT) and a gas gradient to calculate model datum pressure, since the initialisation applied gas down to 3210 m TVDSS. The Midlaren GIIP in the V6 model of 1.2 Bcm was much larger than the 195 mln Nm³ Midlaren GIIP estimate. In the V7 model the Midlaren GWC is lifted to the bottom of the Ten Boer (3173 m TVDSS) and a water gradient used to calculate datum pressure at the correct Midlaren datum of 3190 m TVDSS. The Midlaren fault is set to fully open in both V6 and V7 models. The V7 model requires a small grid block multiplier ($MLA_gbv_mult = 0.25$) to approximately match the Midlaren depletion.

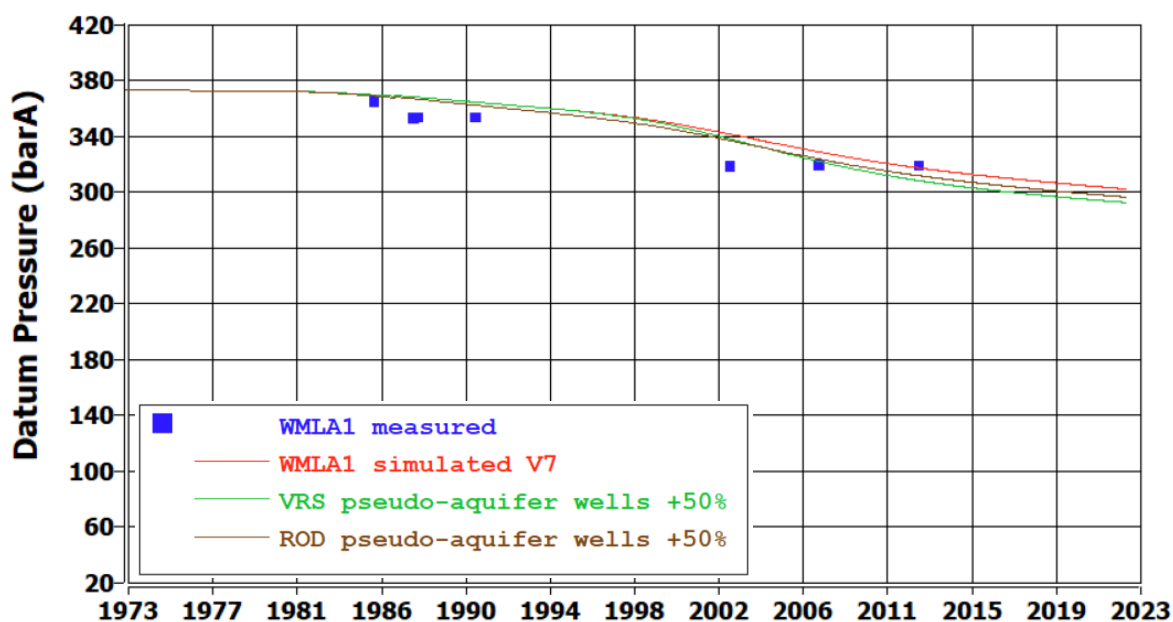


Figure 37: Effect of increasing VRS or ROD pseudo-aquifer well offtake by 50% on simulated MLA-1 pressure.

As discussed in Section 6.6.2, the SPG RMSE for MLA-1 decreases with increased production from Roden and Vries pseudo-aquifer wells. A comparison for these sensitivities is shown in Figure 37. Considering the MLA-1 data uncertainty and flat pressure behaviour since 2002, the V7 model match is considered good enough. The last data point in 2012 is well matched and the forecasted pressure only declines slowly. Though the increased aquifer offtake cases have a lower calculated SPG RMSE they are not considered better.